An Assessment of GEO Orbital Debris Photometric Properties Derived from Laboratory-Based Measurements

Heather Cowardin
ESCG/Jacobs Technology
P.O. Box 58447, Houston, TX 77258-8447y
heather.cowardin@nasa.gov
Kira Abercromby
California Polytechnic State University, Department of Aerospace Engineering
San Luis Obispo 1 Grand Ave, San Luis Obispo, CA 93407
Edwin Barker
NASA Johnson Space Center, 2101 NASA Parkway, Houston, TX 77058
Patrick Seitzer
University of Michigan, Dept of Astronomy
500 Church St, 818 Dennison Bldg, Ann Arbor, Michigan, 48109-1042 USA
Mark Mulrooney
ESCG/MEI Technologies, P.O. Box 58447, Houston, TX 77258-8447
Thomas Schildknecht
Astronomical Institute, University of Bern, CH-3012 Bern, Switzerland

ABSTRACT

Optical observations of orbital debris offer insights that differ from radar measurements (specifically the size parameter and wavelength regime). For example, time-dependent photometric data yield light curves in multiple bandpasses that aid in material identification and possible periodic orientations. This data can also be used to help identify shapes and optical properties at multiple phase angles. Capitalizing on optical data products and applying them to generate a more complete understanding of orbital space objects is a key objective of NASA's Optical Measurement Program, and a primary driver for creation of the Optical Measurements Center (OMC). The OMC attempts to emulate space-based illumination conditions using equipment and techniques that parallel telescopic observations and source-target-sensor orientations. The OMC uses a 75 watt, Xenon arc lamp as a solar simulator, a CCD camera with standard Johnson/Bessel filters, and a robotic arm to rotate objects in an effort to simulate an object's orbit/rotational period. A high-resolution, high bandwidth (350 nm-2500 nm) Analytical Spectral Devices (ASD) spectrometer is also employed to baseline various material types.

Since observation of GEO targets are generally restricted to the optical regime (due to radar limitations), analysis of their properties is tailored to those revealed by optical data products. A small population of GEO debris was recently identified that exhibits the properties of high area-to-mass (A/m) objects (>0.9 m^2/kg), such as variable eccentricities and inclinations, a dynamic characteristic that usually results from variations in solar radiation pressure. In this connection, much attention has been directed towards understanding the light curves of orbital debris and their associated A/m value. Materials, such as multi-layered insulation (MLI) and solar panels, are two examples of materials with high area-to mass ratios. Light curves for such objects can vary greatly, even for the same object under different illumination conditions. For example, specular reflections from multiple facets of the target surface (eg, Mylar or aluminized Kapton), can lead to erratic, orientation-dependent light curves.

This paper will investigate published color photometric data for a series of orbital debris targets and compare it to the empirical photometric measurements generated in the OMC. The specific materials investigated (known to exist in GEO) are: an intact piece of MLI, separated layers of MLI, and multiple solar cell materials. Using the data acquired over specific rotational angles through different filters (B, V, R, I), a color index is acquired (B-R, R-I). As a secondary check, the spectrometer is used to define color indexes for the same material. Using these values and their associated light curves, this laboratory data is compared to observational data obtained on the 1 m telescope of the Astronomical Institute of the University of Bern (AIUB) and 0.9 m operated by the Small- and Medium-

Aperture Research Telescope System (SMARTS) Consortium at Cerro Tololo Inter-American Observatory (CTIO); hereafter noted as the CTIO 0.9 m.

We will present laboratory generated light curves with color indexes of the high A/m materials alongside telescopic data of targets with high A/m values. We will discuss the relationship of laboratory to telescope data in the context of classification of GEO debris objects.

1. INTRODUCTION

A new population of debris in the Geosynchronous (GEO) region possesses high area-to-mass ratios (A/m) [1]. High A/m objects exhibit variable eccentricity and inclination – generally due to the pronounced effect of solar radiation pressure. This high A/m debris population is thought to consist of multi-layered insulation (MLI) or solar panel fragments (solar cells). MLI is a common insulation material found on rocket bodies and spacecraft and is typically composed of reflective, copper-colored Kapton (DuPont manufactured polyimide film) with outer layers of aluminized backing. The interior of the MLI consists of alternating layers of DACRON or Nomex netting with aluminized Mylar.

To aid telescopic identification of such high A/m objects, our laboratory study obtained photometric measurements of multiple MLI samples and solar panel fragments. Of the subset measured, four came from samples of solar panels or intact MLI and two resulted from ground-based hypervelocity impacts on micro-satellites [2]. The targets were illuminated individually with a lamp approximating the solar spectrum and imaged with a CCD camera through Johnson/Bessell [blue (B), visible (V), red (R) and infrared (I)] filters matching the Johnson-Cousins filter system.

We have measured the V-R color index and brightness for these high A/m targets at a fixed phase angle of 8° and at multiple orientations (generally about the .minimum axis of inertia). These data will be compared with observational data from the 1 m telescope of the Astronomical Institute of the University of Bern (AUIB) and 0.9 m telescope operated by the Small- and Medium-Aperture Research Telescope System (SMARTS) Consortium at Cerro Tololo Inter-American Observatory (CTIO); hereafter noted as the CTIO 0.9 m. We have eliminated telescopic observations of objects with large and rapid variations in magnitude (ie, flashers) due to our inability to reproduce this behavior with the current laboratory configuration.

2. DATA ACQUISTION

2.1 Laboratory Photometry

The design of the Optical Measurement Center (OMC) is analogous to a telescope set-up with a light source, target, and observer. A 75 watt, Xenon arc lamp is used to simulate the solar illumination through the spectral range of 200 to 2500 nm. Since certain layers of the MLI saturate the CCD at the lowest time exposure (0.12 seconds), a 0.9 optical, density-neutral density filter was used to reduce the intensity from the source. A simple blackboard covered with black flocked paper is positioned in front of the light source to keep stray light from scattering into the CCD. The data is acquired through a Santa Barbara Instrument Group (SBIG) ST-8XMEI camera, with a front-side illuminated 1024 x 1536 pixels, KAF1602E Silicon CCD. A SBIG CFW8A 5-position filter wheel is attached to the CCD camera. The laboratory uses Johnson/Bessell filters, although Johnson/Cousins have relatively the same bandpasses. The Blue (B) filter bandpass covers the 350-600 nm range, the Visible (V) filter ranges from 450-700 nm, the Red (R) filter ranges from 560-1060 nm, and the Infrared (I) filter covers 700-1100 nm. A telephoto zoom lens is attached to the CCD, enabling manual focusing and magnification of targets. The phase angle is that made between the source, target, and CCD camera and is set to 8° ± 1° for all the data taken for this paper. On-going measurements use higher phase angles (max of 60°), but will not be discussed in this paper. An ST-Robotics R17 5-axis articulated arm robot, on loan from the Air Force Research Laboratory in Maui, is used to rotate objects through five degrees of freedom (base rotation, shoulder, elbow, wrist, and wrist rotation). A layout of the laboratory is seen in Fig. 1. The target, a sample of glass fiber-reinforced plastic fragment (GFRP), is shown in the near view on the right side of the figure, is nearly 4 m away from the source and less than 3 m from the detector.

Fig. 1. The layout from the robot's perspective of the OMC at an 8° phase angle

2.2 Samples Investigated

In Table 1, the materials investigated are shown with their respective A/ms. Objects with A/m >0.9 m^2/kg are considered high A/m targets. The MLI intact is covered with copper-colored material on both faces, one side space facing and the other spacecraft facing. Separating these two layers of the intact MLI, the space facing layer has a higher A/m than the spacecraft layer, which is interwoven with thread, slightly adding to the mass of the target. The MLI complex target is a remnant of microsatellite ground collision that appears intact, but the interior layers are visible. Unlike the former targets that are held taunt with simple black materials, the complex MLI target is mounted by the only intact threaded side, allowing the layers to fan out and move during rotations. The solar cell fragment is also a result of the microsatellite ground collision, in which only the solar cell material and backing is visible. The intact solar panel fragment is from a sample solar panel, courtesy of NASA's Jet Propulsion Laboratory, which is composed of standard solar panel material with gallium arsenide solar cells. The sample is thought to be roughly 5 to 6 years old. The bottom is composed of carbon fiber-reinforced plastic (CFRP) and the interior is an aluminum, honeycomb material.

Table 1. List of laboratory targets investigated

Target Material	A/m (m^2/kg)
MLI intact	2.1
MLI space-facing layer	5.43
MLI spacecraft-facing layer	4.15
MLI complex (Kyushu University)	3-4
Solar cell fragment (Kyushu University)	1.00
Intact solar panel fragment	0.5

2.3 Telescopes

The CTIO 0.9 m telescope is located inland from La Serena, Chile and is used to acquire photometric measurements for the NASA Orbital Debris Program Office. It can track satellites at their angular rates up to 2° per sec in right ascension, and has a 0.22° field of view (fov). The data is acquired through standard Johnson/Bessell B, V, R, and I filters.

Data published from the European Space Agency (ESA) 1 m telescope of the Astronomical Institute of the University of Bern (AIUB), located in Zimmerwald, will be used as a secondary comparison for laboratory data. The data is acquired through Johnson/Cousins BVRI bands. The data to be compared from this instrument is, primarily, published photometric light curves of high A/m populations located in the GEO regime.

3. MEASUREMENTS

3.1 Laboratory-based Measurements

Laboratory-based photometry [3], when correlated with telescopic observations, may enable identification of material types. To this end, we have acquired BVRI photometry data of various targets (Table 1) at orientations incremented by 10° over a 360° rotation. Since we are correlating with GEO observations taken near the anti-solar

point, we have fixed the phase angle at 8° ± 1°. As will be shown, the measured color indices and orientation-dependent light curves, when compared with telescopic data, are indeed indicative of orbiting material type.

In the figures below, the color plots show the two maximum cross-sectional areas for each object with the background removed; red pixels indicate high intensities and blue pixels indicate low intensities (ie, same value as the background). In the case of the intact solar panel, the side view is shown as well, since it is not a thin plate-like shape. The middle plot shows the V-R color index for each object (rather than B-R, which was subject to poor signal-to-noise at certain orientations). Discontinuities in the color index plots is an artifact arising when signal in a given filter dropped to near background levels. The ordinate indicates the visible to red magnitude ratio, where positive numbers indicate a higher magnitide in the R filter and negative numbers a higher magnitude in V. The abscissa shows the orientation angle ranging from 0° to 360°.

The MLI-intact piece is shown in Fig. 2, with the spacecraft facing surface (left) visible in the first half of the rotation and the space facing layer visible in the later half (right). The middle figure shows the V-R plot, which is positive over the majority of the rotation, indicating the material is more reflective in the red than the visible. This is expected with Kapton material, which has poor V reflectivity due to a strong absorption feature near 480 nm [3]. The peak seen near 180° is due to a glint from the interior layers of the MLI, which have a stronger reflectance in the V and B relative to the R.

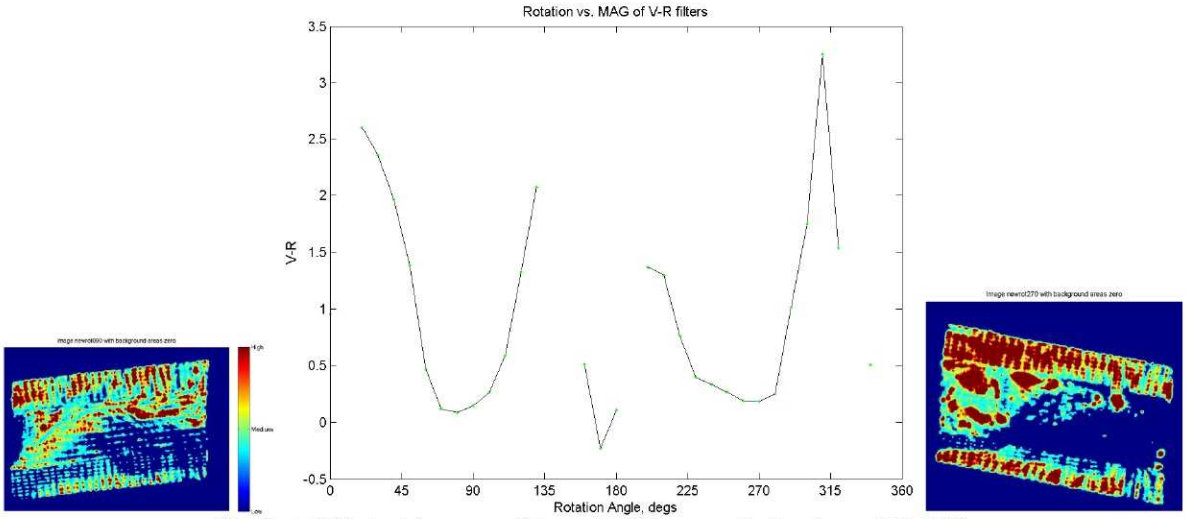

Fig. 2. MLI intact (spacecraft layer 0-180, space-facing layer 190-360)

The space-facing and spacecraft facing MLI layers are shown in Fig. 3 and Fig. 4, respectively. The first half of the rotation for the space-facing layer has the aluminized Kapton layer (referred to as "silver" in the captions) illuminated, followed by the copper-colored Kapton layer (referred to as "copper" in the captions) in the later half. The opposite arrangement applies to the spacecraft-facing layer, where the copper-colored Kapton is first illuminated, followed by the aluminized Kapton layer. Both targets show the copper-colored Kapton is more reflective in the R filter and the aluminized Kapton in the V filter. The notable difference is the structure of the light curves, where the woven spacecraft-facing layer has a smoother plot structure compared to the space-facing layer [3]. Due to the structure of the space-facing layer, the material is not able to support itself and is free to curl orbend under the natural weight of gravity. This non-rigid shape allows for multiple glints over the rotation sequence and is not easily repeatable from one rotation to the next.

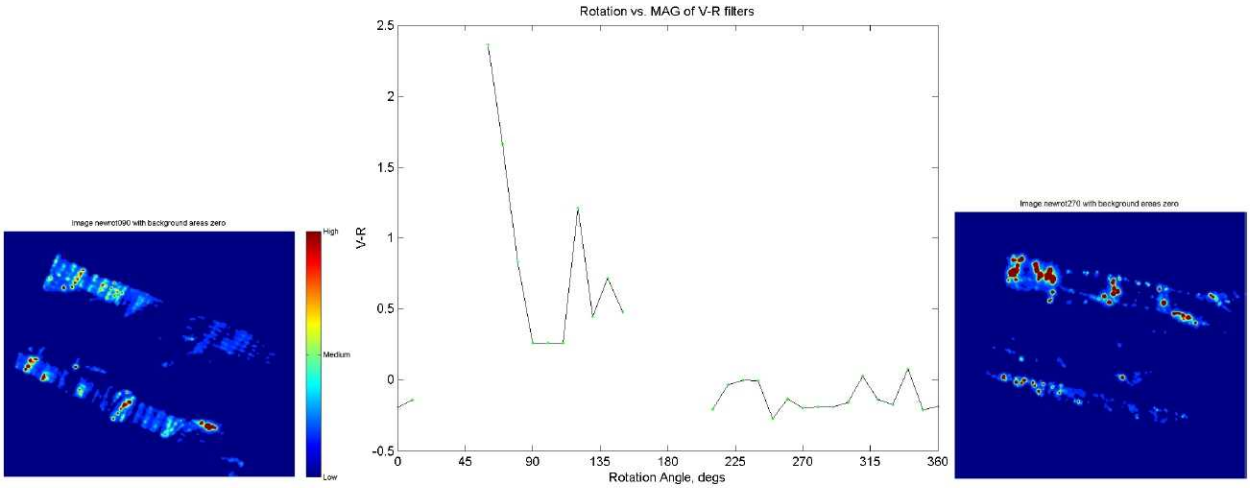

Fig. 3. Space-facing MLI layer (copper 0-180, silver 190-360)

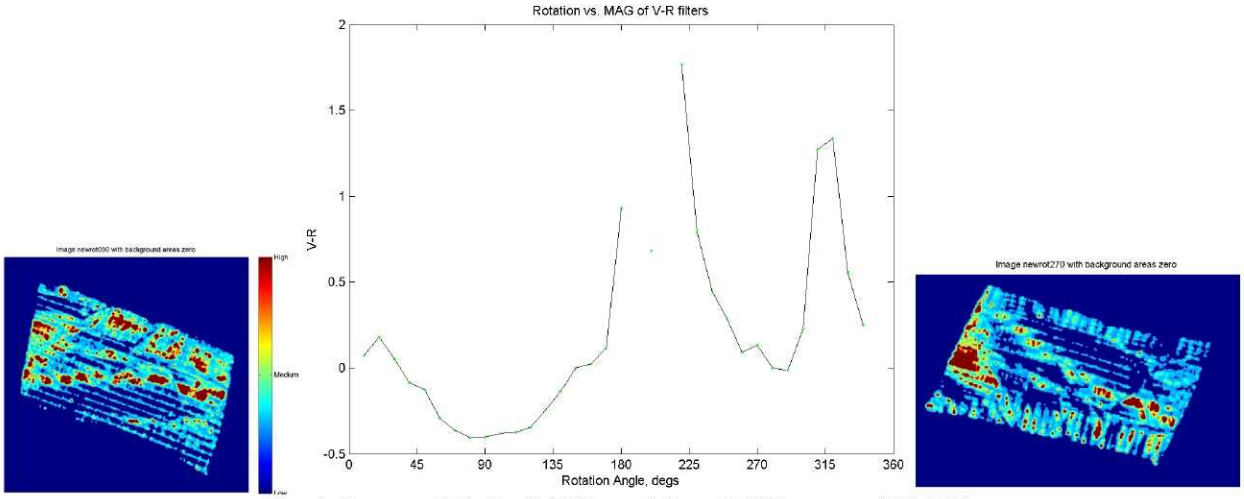

Fig. 4. Spacecraft facing MLI layer (silver 0-180, copper 190-360)

In Fig. 5 the MLI complex fragment is shown. The copper-colored polyimide film is visible at both faces, but has torn, allowing the different interior surface layers to be illuminated. The copper-colored polyimide film appears to have burn marks and, possibly soot, covering the exterior layers due to the impact, which ultimately reduced the total possible reflectance. An example of this is seen in the left color plot; the dark blue area covering the maximum surface area is copper-colored polyimide film, but due to the film covering the surface, the reflectance is reduced to nearly zero.

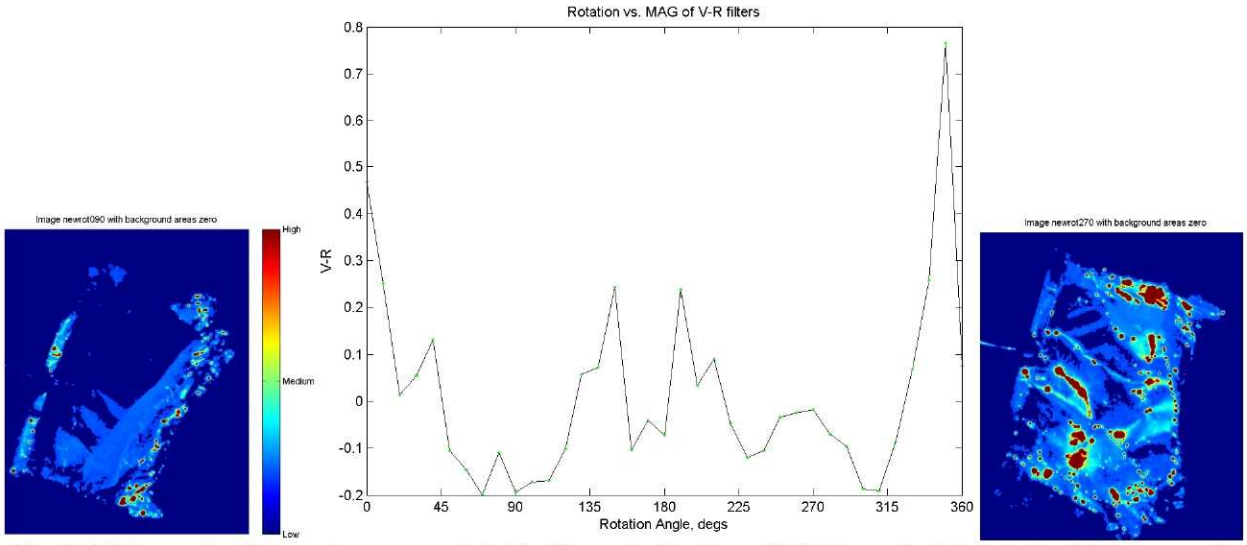

Fig. 5. MLI complex fragment, copper polyimide film on both sides with Mylar and white interior fabric exposed.

The solar panel fragment was oriented with the first half of the rotation illuminating the backside of the fragment (aluminum) and the later half showing the solar cell material, as shown in the left and right color plots of Fig. 6, respectively. The bright red area on the right-hand color plot indicates areas where the solar cell material has fragmented, allowing for the underlying material to be exposed. The V-R color index plot shows that the target is more reflective in the V filter throughout the entire rotation.

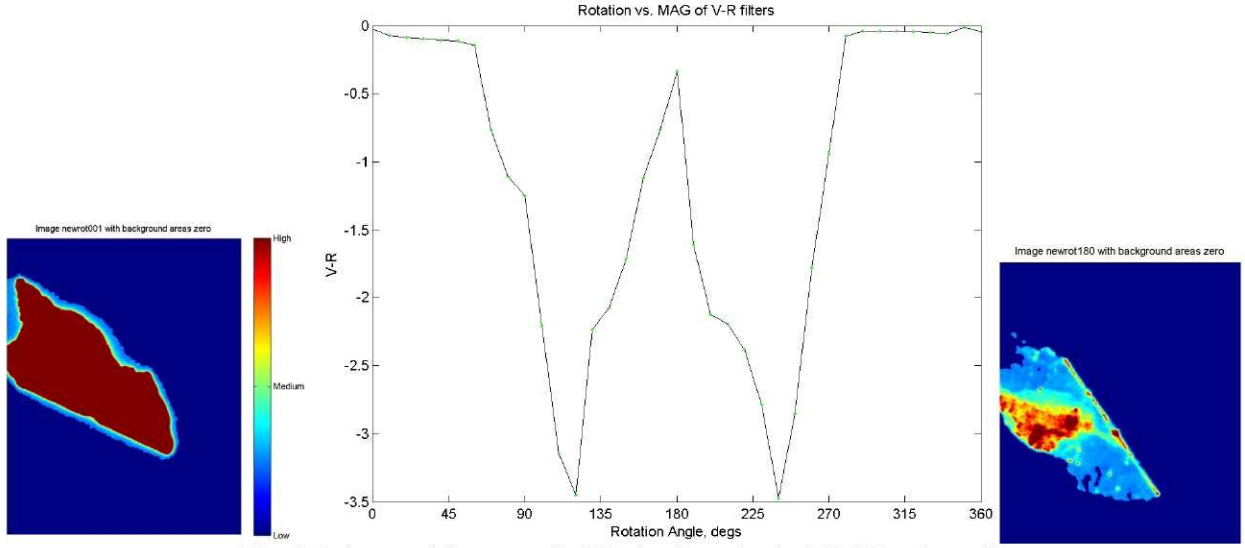

Fig. 6. Solar panel fragment (0-170 aluminum back, 180-350 solar cell)

In Fig. 7 the peaks in the V-R color index plot are dependent on the material surface area that was visible at each specific orientation. The first andlast peaks between 0°-90° and 280° -360°, occurred when the solar cell side was visible (first color plot). The troughs around 90° and 270° refer to when the honeycomb, aluminum interior was oriented to the detector. The second trough at 180° is due to the CFRP visibility (shown in the last color plot). The two peaks near 140° and 220° indicate orientations where the magnitude was higher in the V than the R by nearly a magnitude. Even with the differently-illuminated materials, the plot indicates the material is more reflective in the V filter.

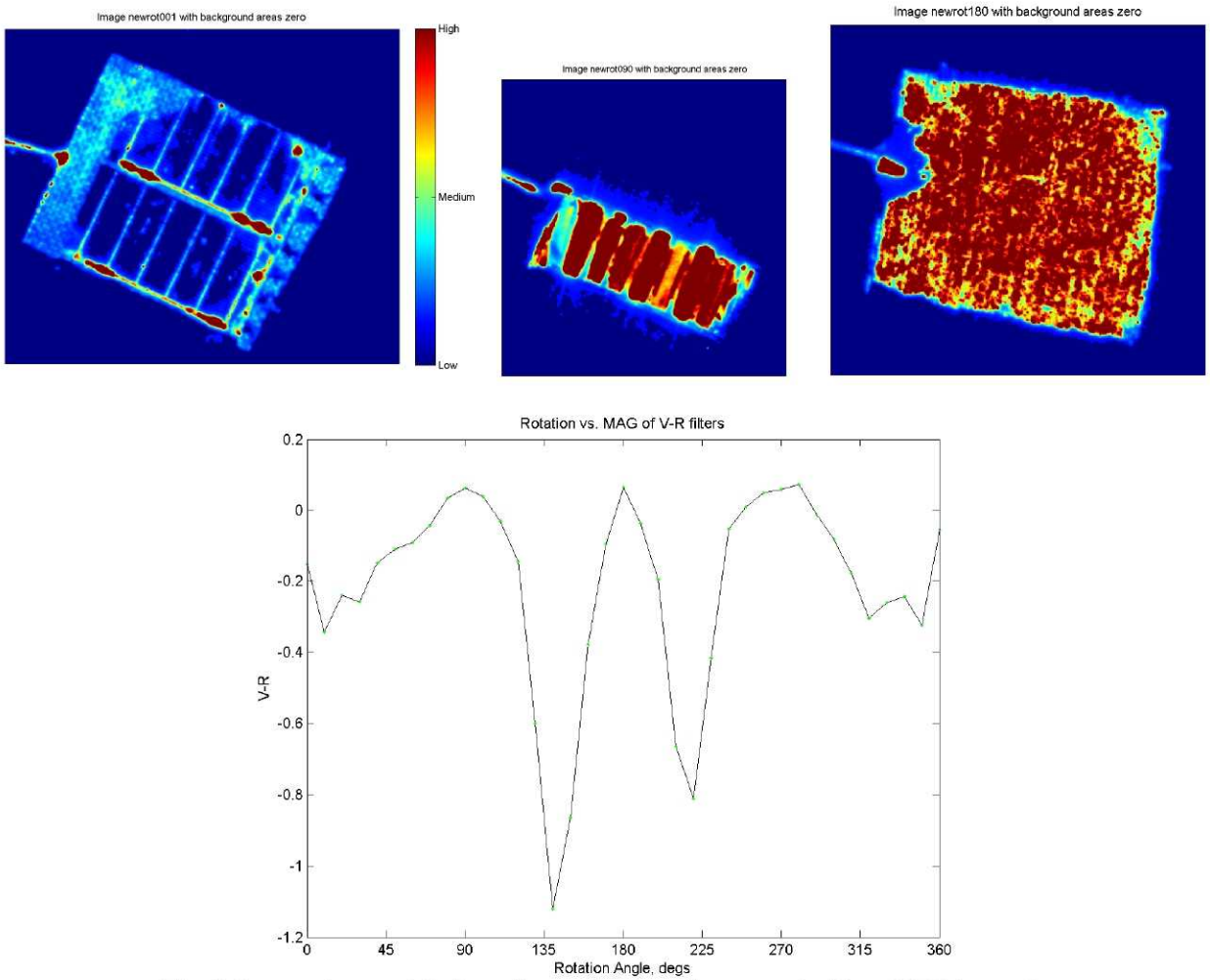

Fig. 7. Intact solar panel (solar cell top, aluminum honeycomb sides, CFRP bottom).

3.2 Telescope-based Measurements

For details on how telescope measurements are acquired, consult references 1, 4, and 5. This section will show light curves of GEO orbital debris acquired through the two telescopes mentioned in Section 2.2. Published telescope data from T. Schildknecht of AIUB are shown in Fig. 8; both light curves refer to the same bright object with a respective A/m = 1.9 m^2/kg [5]. The primary periodicity for both cases is approximately 1-2 minutes. Attempting to compare laboratory light curves to those of space objects acquired over several days has proven to be impossible. As a specific example, the variations due to object glinting (with sharp increases/decreases on the order of ~5 magnitudes) prevents direct comparisons. Since glinting is common to both MLI and solar cell fragments, one must use the color indices to gain a better knowledge of the material. With the known physical characteristics of fragments in the laboratory, one can compare the A/m from telescope observations and A/m with ground-test fragments to find the best match. Based on the calculated A/m for the MLI-intact sample and the solar cell fragment, the telescopic data would likely best match one of these samples (see Fig. 2 and Fig. 6, respectively). The magnitude variations on the telescope data appear to be on the order of six on the initial graph and approximately one to one and a half on the following plot. The variations for the laboratory data are dependent on the filter used. For the solar panel fragment, the magnitude range between peaks was approximately 7 for B and V, and 9 for R. The intact MLI, target magnitude range was approximately 9 and 11 in the R and I filter, respectively.

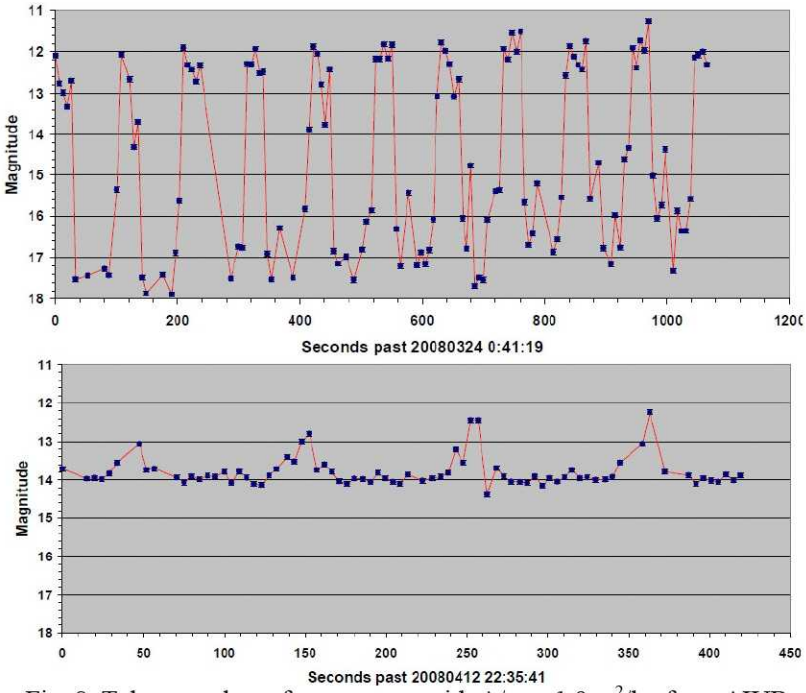

Fig. 8. Telescope data of same target with A/m = 1.9 m^2/kg from AIUB

The following data (Fig. 9) was taken with the CTIO 0.9 m. The object in Fig. 9 was determined to be an uncorrelated target (UCT) not catalogued by the U. S. Space Surveillance Network. Due to the lack of magnitude variations within the 5- to 20- minute observing sequence, all data points shown are defined as stable. The filter photometry is taken in the following sequence: R:B:I:V:R, always starting and finishing the sequence with the red filter to investigate any systematic change over the (~20 minutes) of the entire observation set. The plot shows the magnitudes for each filter as a function of UT (decimal hour). Starting with the top left image of Fig. 9 and moving clockwise, the R, B, V and I magnitudes are plotted. The initial R measurement is shown in red and the last R measurement is shown in magenta. Some data points are missing due to contamination by star streaks. This object shows very small brightness and color variations in all filters for all short time scales (5 - 20 minutes), suggesting we are seeing just one aspect of this piece of debris. However, on longer timescales, both brightness and colors change significantly (note the behavior near 3 hours UT), where the object brightens in B by 3 magnitudes (15 x), yet becomes fainter in I by about the same amount. This type of behavior is also seen in the OMC with the layered MLI when the copper-colored Kapton rotates towards the aluminized Kapton face, which changes from peaking in the R to peaking in the B or V, respectively.

Does this large change in B-I reflect a true change in the observed surface, or was there a sudden change in surface or orientation between when the B and I observations were obtained near 3 h UT? Sequential observations in different filters are fundamentally unable to answer this question, and so we have begun a program to obtain simultaneous measurements of the same object in two different filters. The CTIO 0.9 m observes in B, while the Michigan Orbital DEbris Survey Telescope (MODEST), also located at Cerro Tololo Inter-American Observatory (CTIO), observes in R. The MODEST CCD camera is electronically synced to the CTIO 0.9 m CCD camera, so both exposures have the same start time and duration to better than 50 milliseconds. Details of these experiments will be reported at the AMOS 2009 Technical Conference [4].

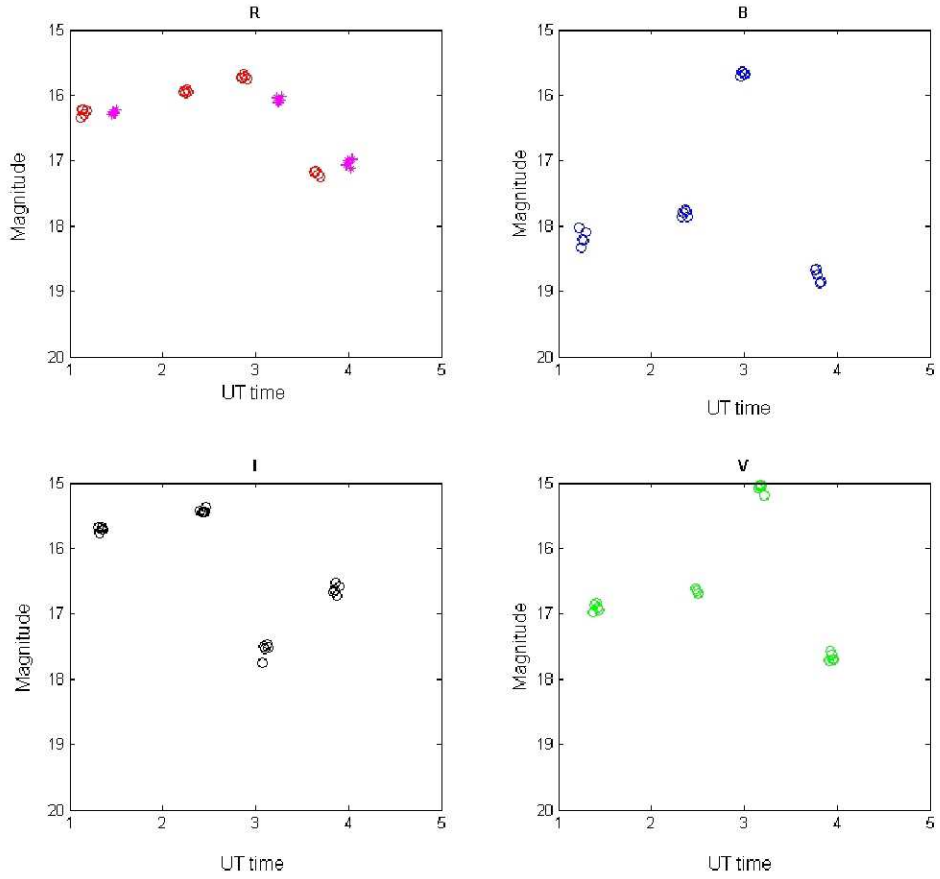

Fig. 9. Photometry of stable UCT from CTIO 0.9 m

4. CONCLUSIONS AND FUTURE WORK

Both laboratory color and A/m measurements can be used to help determine the material composition of orbital debris that are observed with ground-based optical telescopes. With this information, the laboratory attempts to emulate a fragment drifting in space. Using mounting techniques that would preserve the fragment, the minimum axis of rotation was selected, although it is understood this axis is not equivalent to actual space debris. The photometry; however, still provides a glimpse of the actual light curve for known materials and sizes. The initial phase angle was set at 8° ± 1° and will soon be extended to both 30° and 60° to best replicate the phase angles of other telescope observations.

It was concluded the A/m is not sufficient to determine material type. Although the A/M for the AIUB fragment best matches the laboratory value for MLI, there are other materials (such as solar cell fragments) which also have similar A/m values. The fragment observed at CTIO was stable enough to measure the color indices, but these indices were observed to change when measured over a period of several hours. The color changes were consistent with laboratory measurements of MLI when the aluminized Kapton becomes illuminated. The current one- or two-telescope operations require that colors be measured sequentially. The measured debris must be stable over the time period needed to sequence through the filters. Lastly and surprisingly, the fragments studied until recently, have all been samples in relatively good condition, but the MLI fragment from the hypervelocity impact showed that the reflectance is reduced significantly due to the collision, leaving a thin film of suspected dark soot over the surface. This could imply that explosions in space that involve MLI may be undetectable at certain orientations.

Although there are multiple materials in the laboratory that have high A/m (eg, GFRP and CFRP), their photometric light curves were smooth, lacking multiple glints, and unlikely to match the telescopic data shown in this paper.

Acquiring the same amount of data from both sources is the key to making a firm conclusion on suspected target correlations.

As we move forward, we intend to provide an expanding database of light curves and color indices at different phase angles and orientations thought to best represent spacecraft material types. We will continue to look for correlations to telescopic observations, with the intent of the assessing the material characteristics of the orbital debris population and the threat posed.

5. ACKNOWLEDGEMENTS

I would like to thank Gary Foreman with the University of Michigan for his hard work reducing all the photometry data from the CTIO 0.9-m telescope. The photometric observations of debris reported in this paper were obtained largely on the CTIO 0.9 m telescope, which is operated by the SMARTS consortium. We thank the SMARTS Director, Prof. Charles Bailyn of Yale University, and the entire consortium for granting us access to this telescope at the times that were most beneficial to us. Special thanks to the Air Force Research Laboratory in Maui for loaning the robotic arm to NASA\JSC. Lastly, thanks to Jasvir Singh, from San Jose State University in California, for his help with setting up the new laboratory, and to Jacqueline Heard and Jonathon Daniels, both from Prairie View A&M University, who acquired numerous laboratory photometric measurements that helped make this paper possible.

6. REFERENCES

1. Schildknecht, T., et al, Properties of High Area-to-Mass Ratio Space Debris Population in GEO, 2005 AMOS Technical Conference Proceedings, Kihei, Maui, HI, 2005.
2. Hanada, T. and Liou, J.C., Comparison of fragments by low- and hyper- velocity impacts, Advances in Space Research, Vol. 41, 1132-1137, 2008.
3. Rodriguez, H., et al, Optical Properties of Multi-Layered Insulation, 2007 AMOS Technical Conference Proceedings, Kihei, Maui, HI, 2006.
4. Seitzer, P., et al, Photometric Studies of GEO Debris, 2009 AMOS Technical Conference Proceedings, Kihei, Maui, HI, 2009, *in preparation for this conference.*
5. Schildknecht, T., et al, Color Photometry and Light Curve Observations of Space Debris in GEO, 2008 International Astronautical Congress, Glasgow, Scotland, October 2008.

An Assessment of GEO Orbital Debris Photometric Properties Derived from Laboratory-Based Measurements

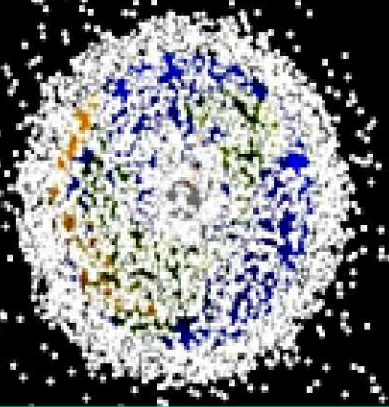

Heather Cowardin

ESCG/Jacobs Technology, University of Houston

heather.cowardin@nasa.gov

Kira Abercromby, Ed Barker, Patrick Seitzer, M. Mulrooney, & T. Schildknecht

Outline

- Introduction
- Equipment and telescopes used
- Laboratory photometry measurements
- Comparison to telescopic- and laboratory- acquired data
- Conclusions and future work

Background

- **Focus**
  - Orbital debris detection in the GEO regime
  - Concentration on objects with high A/m
  - Laboratory materials discussed: Solar panel, MLI, and fragmentation debris of both materials
  - Telescopic photometry gives insight into object's material type, and possible shape/orientation over time

- **Goal**
  - Using laboratory-produced light curves, one can compare light curves to actual space debris in hopes of better understanding GEO environment
  - Ultimately a model will be in place to better define the GEO environment based upon material, shape, size, and postulated rotation

Optical Measurement Center (OMC)

- **Part of the Orbital Debris Program Office located at NASA\JSC in Houston, Texas**

- **Equipment used**
  - Source
    - 75 W Xenon arc source
  - CCD
    - SBIG ST-8XMEI, KAF1602E, 1024x1536 pixels
  - Filters
    - Johnson/Bessell BVRI
  - Robotic Arm:
    - ST-Robotics R17 5-axis articulated arm robot
  - Moveable optical bench
    - Used to move CCD camera to acquire multiple phase angles (0°-60°)

OMC layout

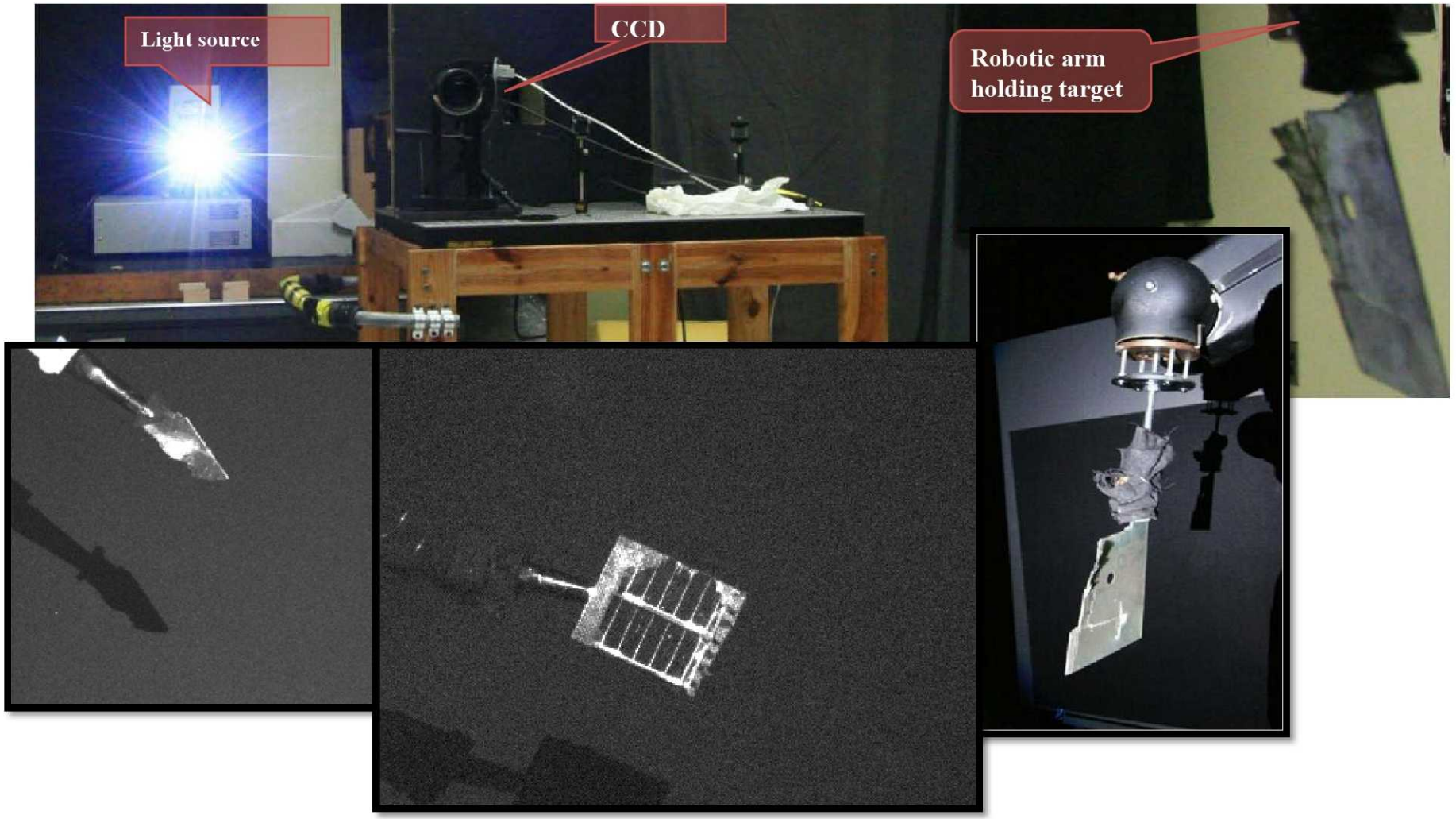

Cerro Tololo Inter-American Observatory (CTIO) 0.9 m

- Located inland from La Serena, Chile
- 0.9-m Cassegrain
- 0.22 deg FOV
- 0.792 arc-seconds/pixel
- Blue sensitive CCD
- BVRI filters
- Track objects at their angular rates

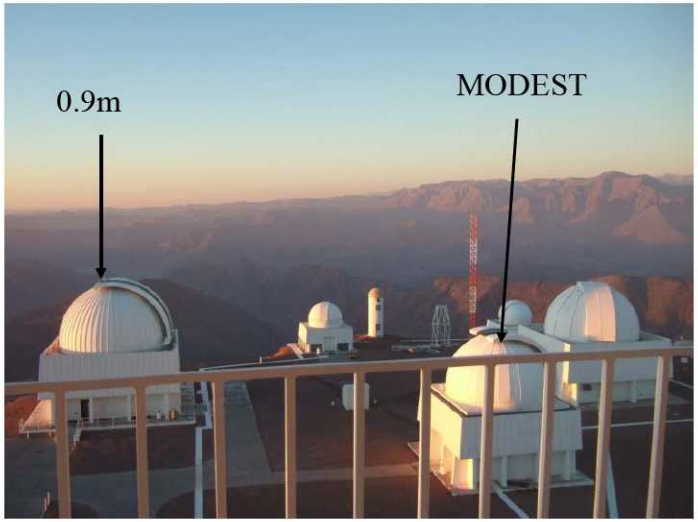

ZIMLAT 1 m telescope of AIUB's Zimmerwald observatory

- European Space Agency (ESA) 1 m telescope of the Astronomical Institute of the University of Bern (AIUB)
- Located in Zimmerwald
- Ritchey-Chrétien telescope
- 0.35 degree FOV
- 0.7 arcsec/pixel
- BVRI filters


Laboratory Measurements

Sample Target Orientation/Rotation: Intact

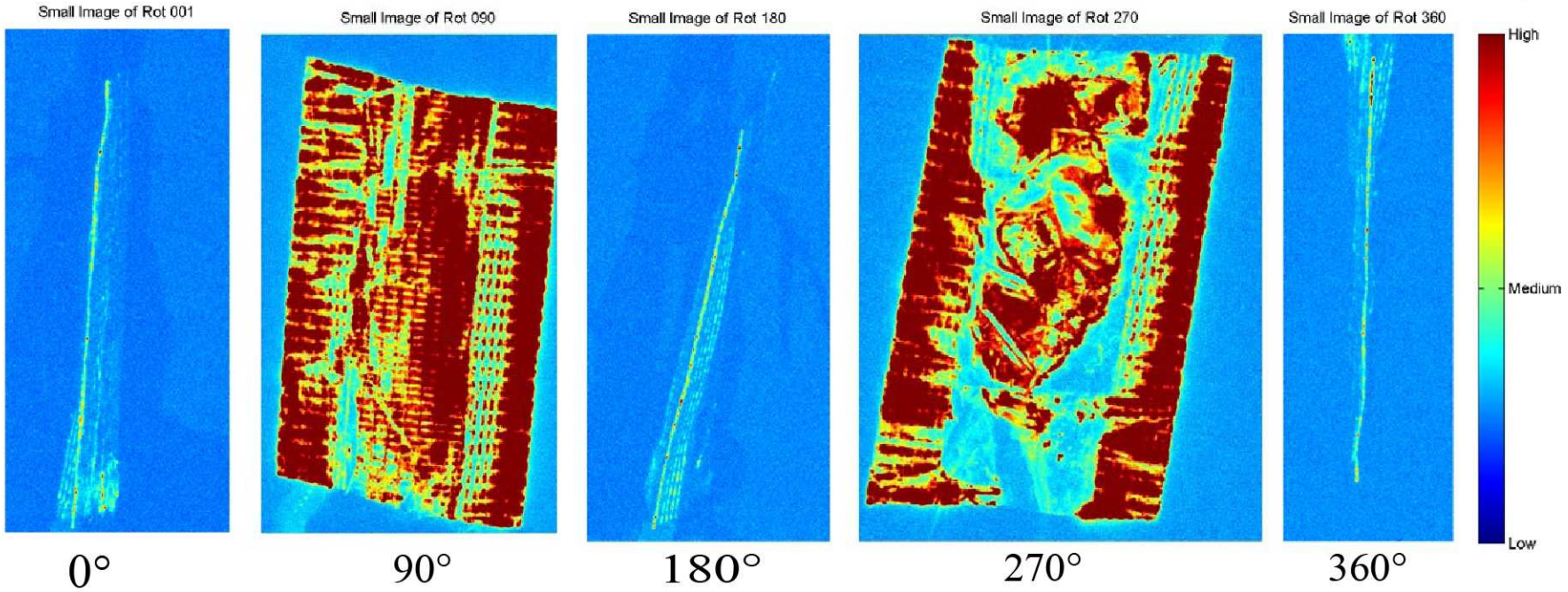

- **0°: partial view of spacecraft facing and space facing**
- **90°: normal reflection to spacecraft-facing Kapton**
- **180°: partial view of spacecraft facing and space facing**
  - object appears flipped as target was rotated on rotary table to compensate for full 360° due to prior robotic arm limitations
- **270°: normal reflection from space-facing Kapton**
- **360°: theoretically should be exactly the same as 0°, except image is flipped upside down**

Targets

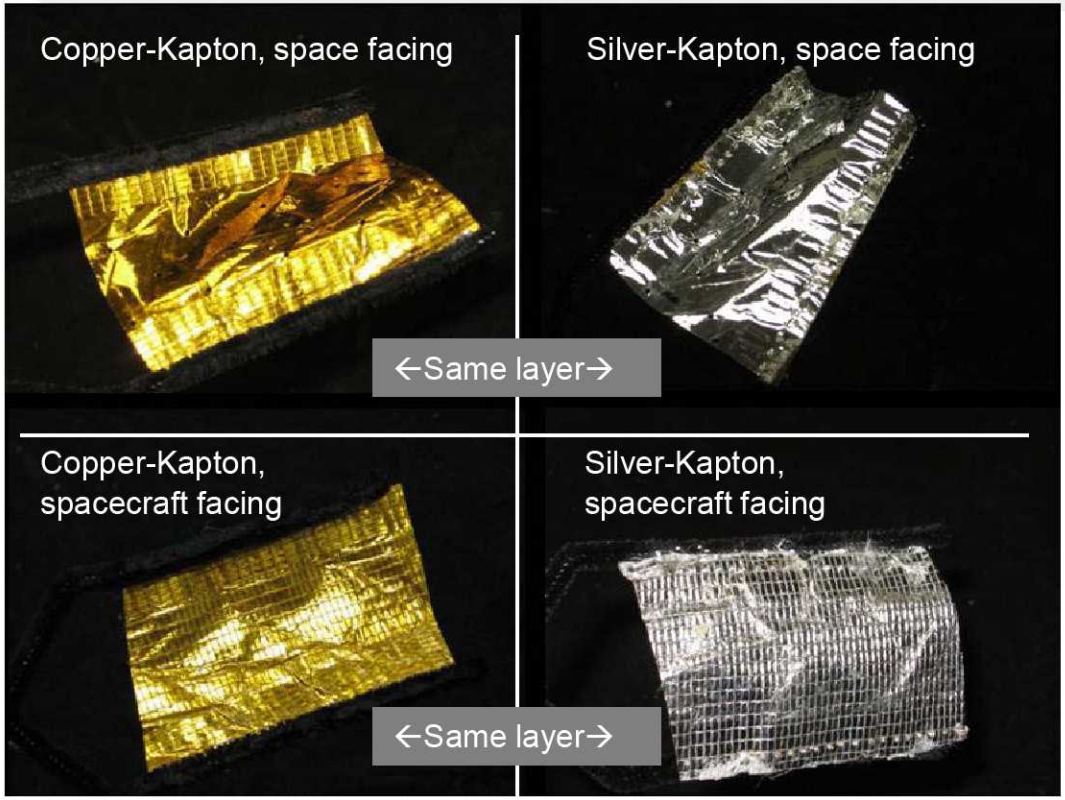

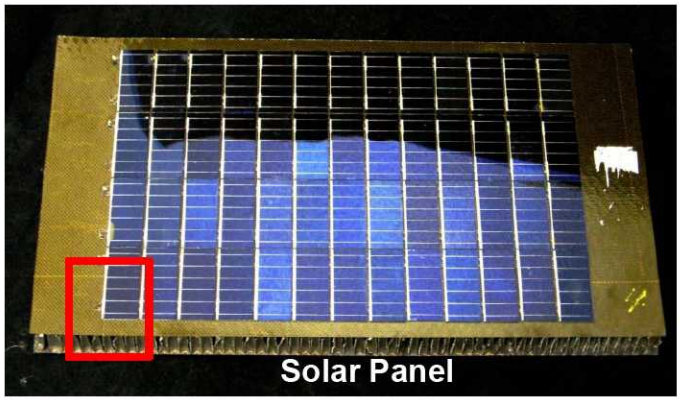

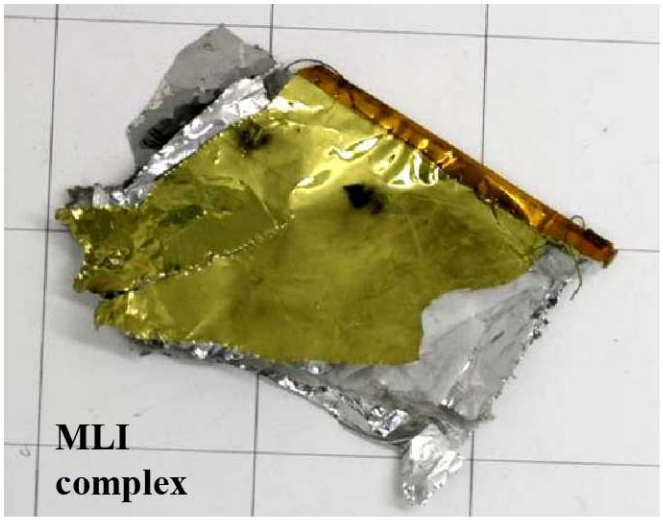

Target Material	A/m (m^2/kg)
MLI intact	2.1
MLI space-facing layer	5.43
MLI spacecraft-facing layer	4.15
MLI complex (Kyushu University)	3-4
Solar cell fragment (Kyushu University)	1.00
Intact solar panel fragment	0.5

B-V Color Index as a Function of Rotation Angle as Measured from the Laboratory CCD

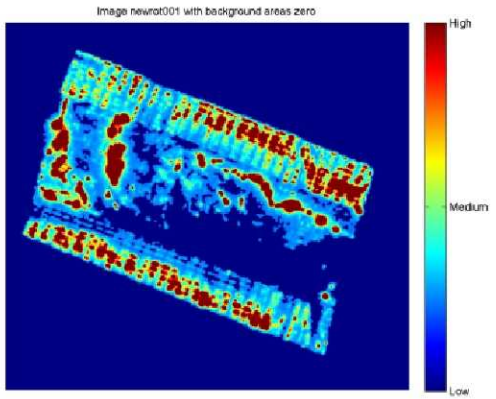

Intact MLI

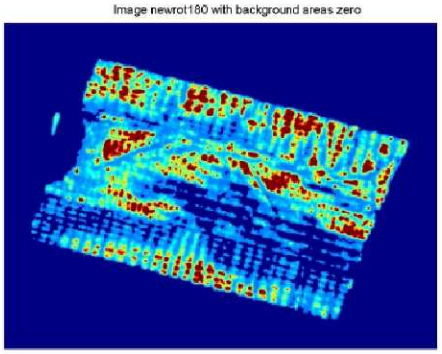

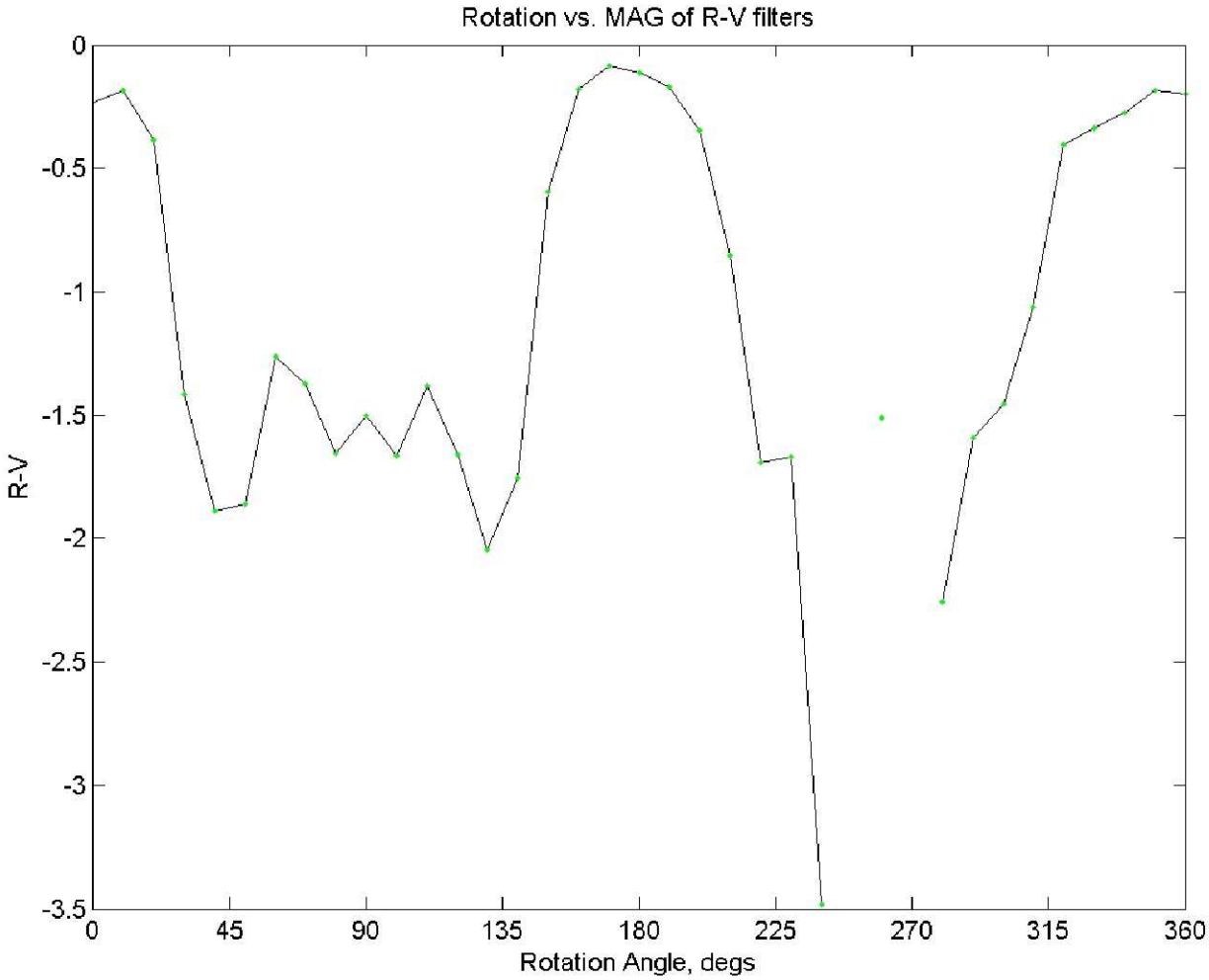

Intact movie

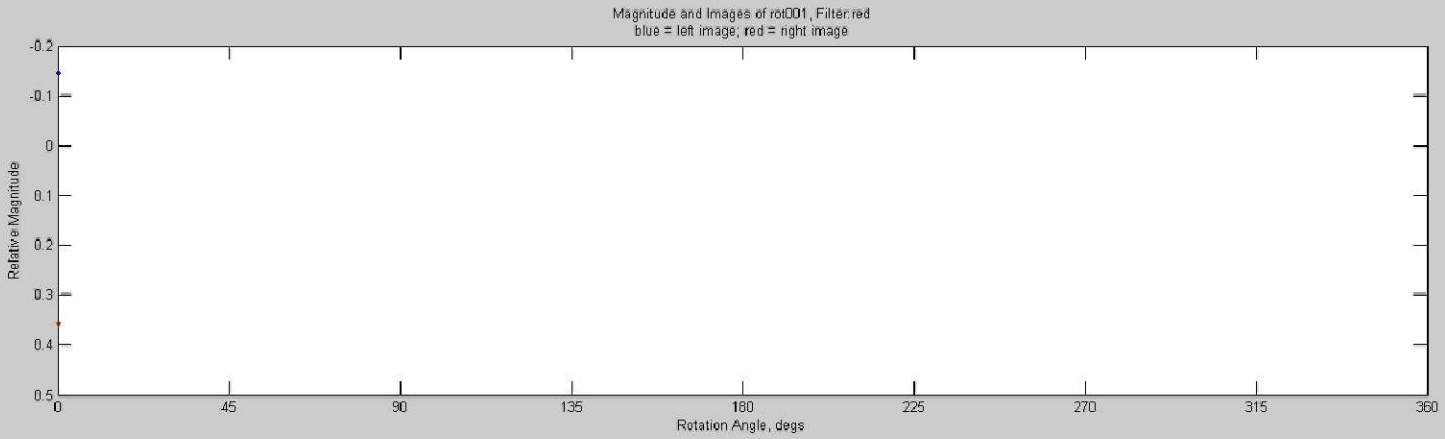

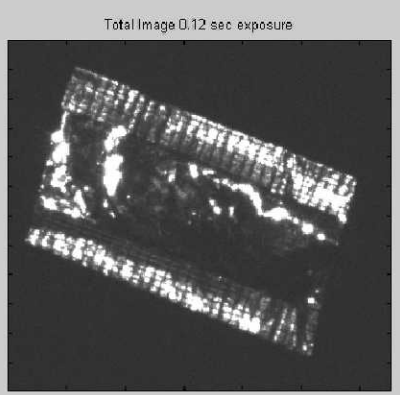

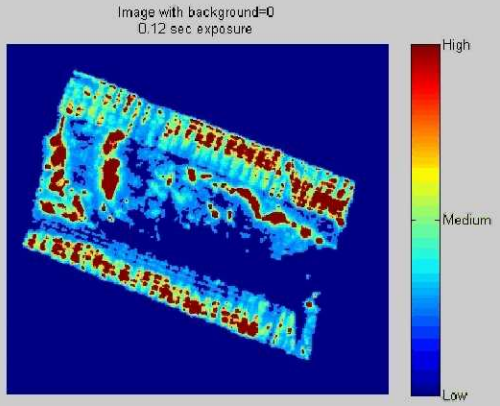

MLI complex fragment

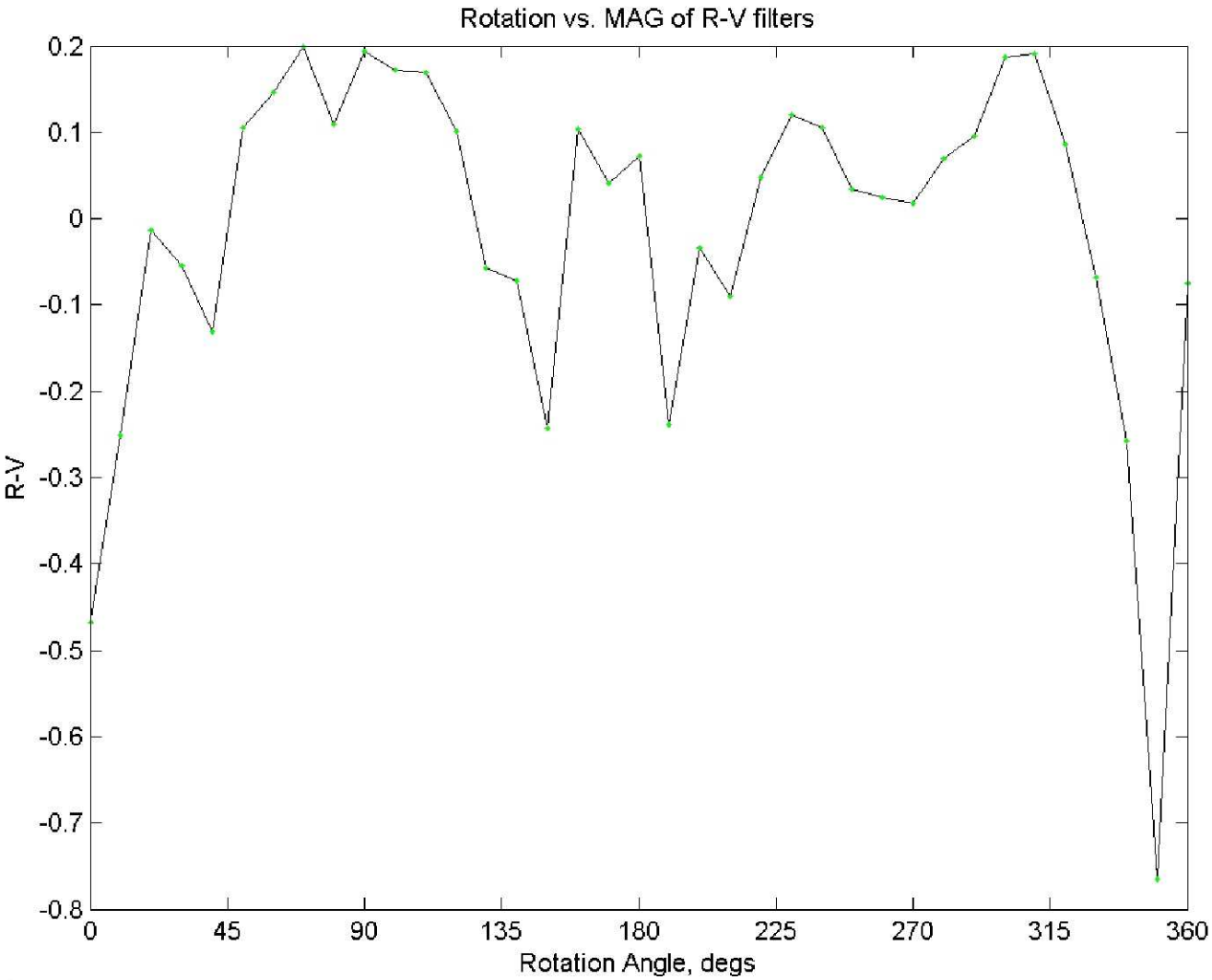

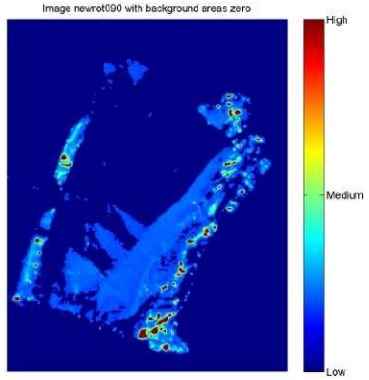

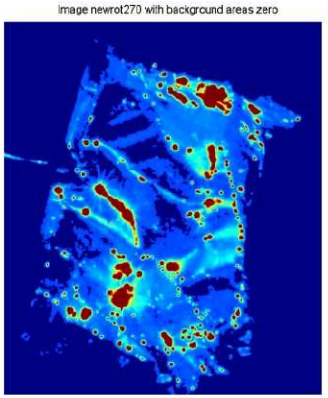

MLI complex fragment

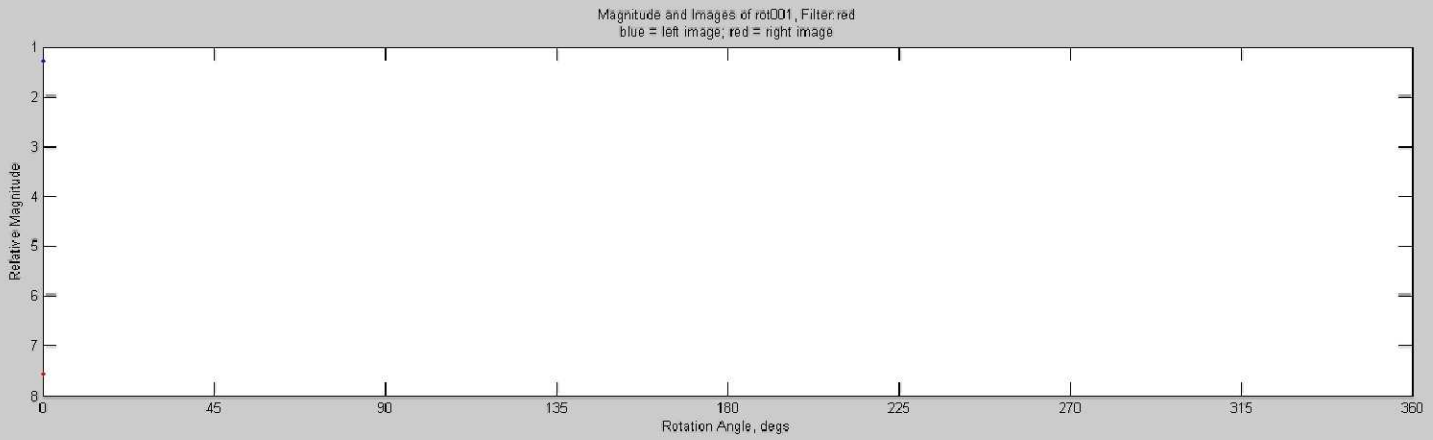

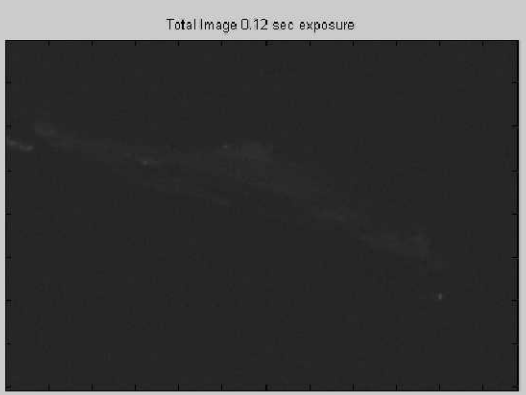

Space-facing and Spacecraft-facing MLI layers

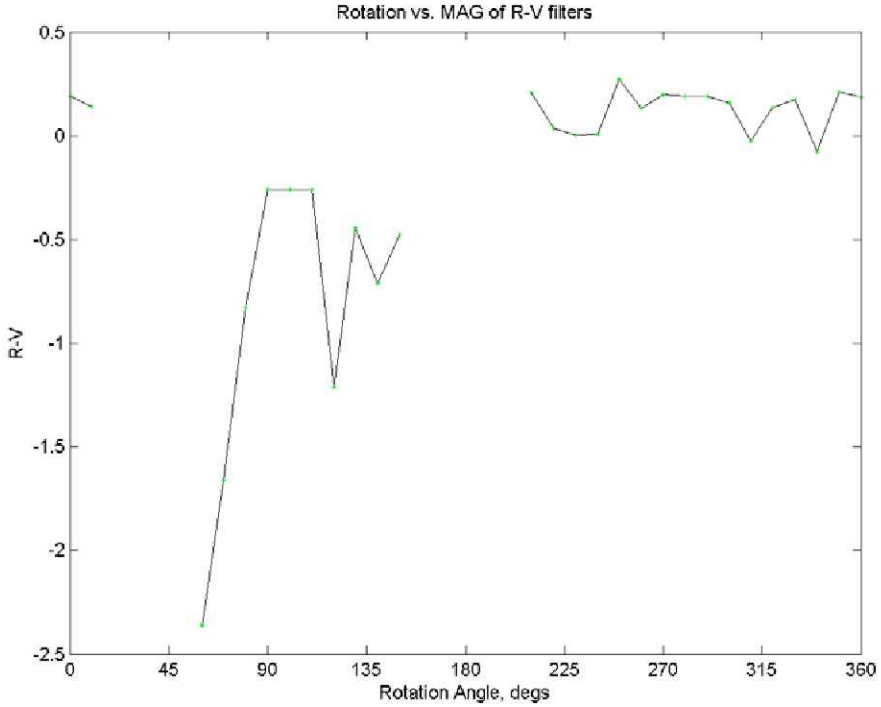

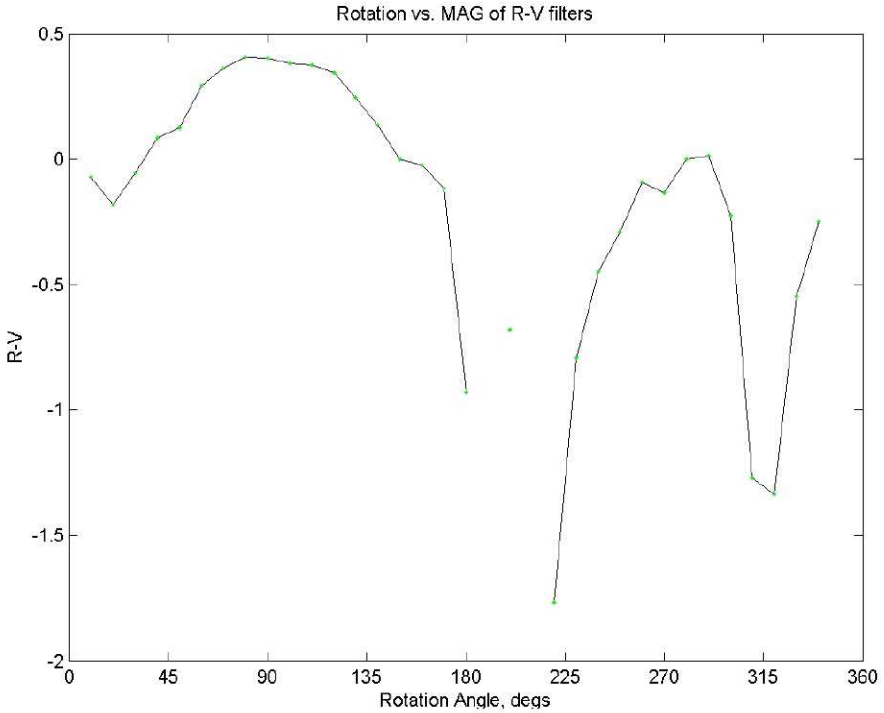

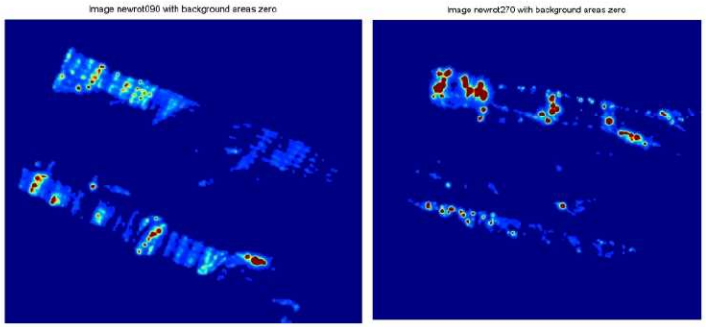

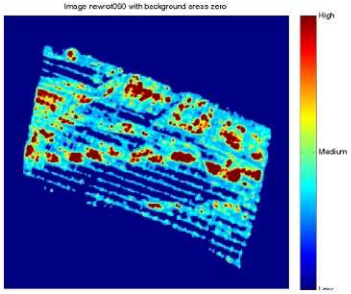

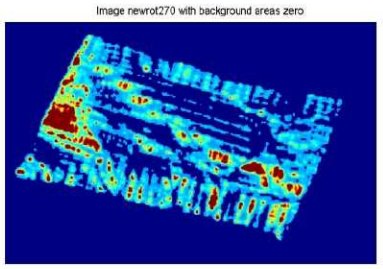

MLI layers: spacecraft-facing top, space-facing bottom

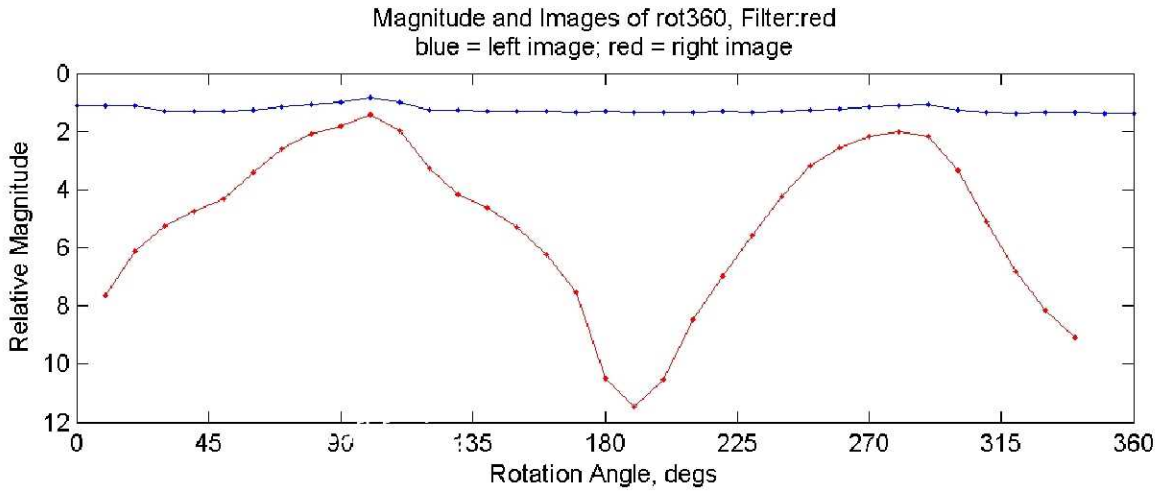

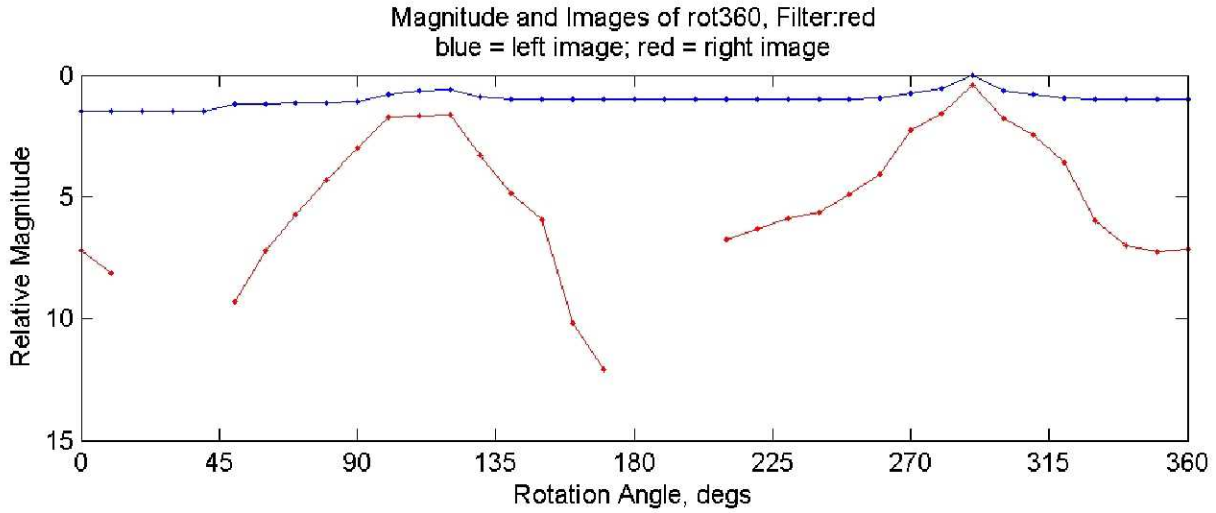

Solar Cell fragment

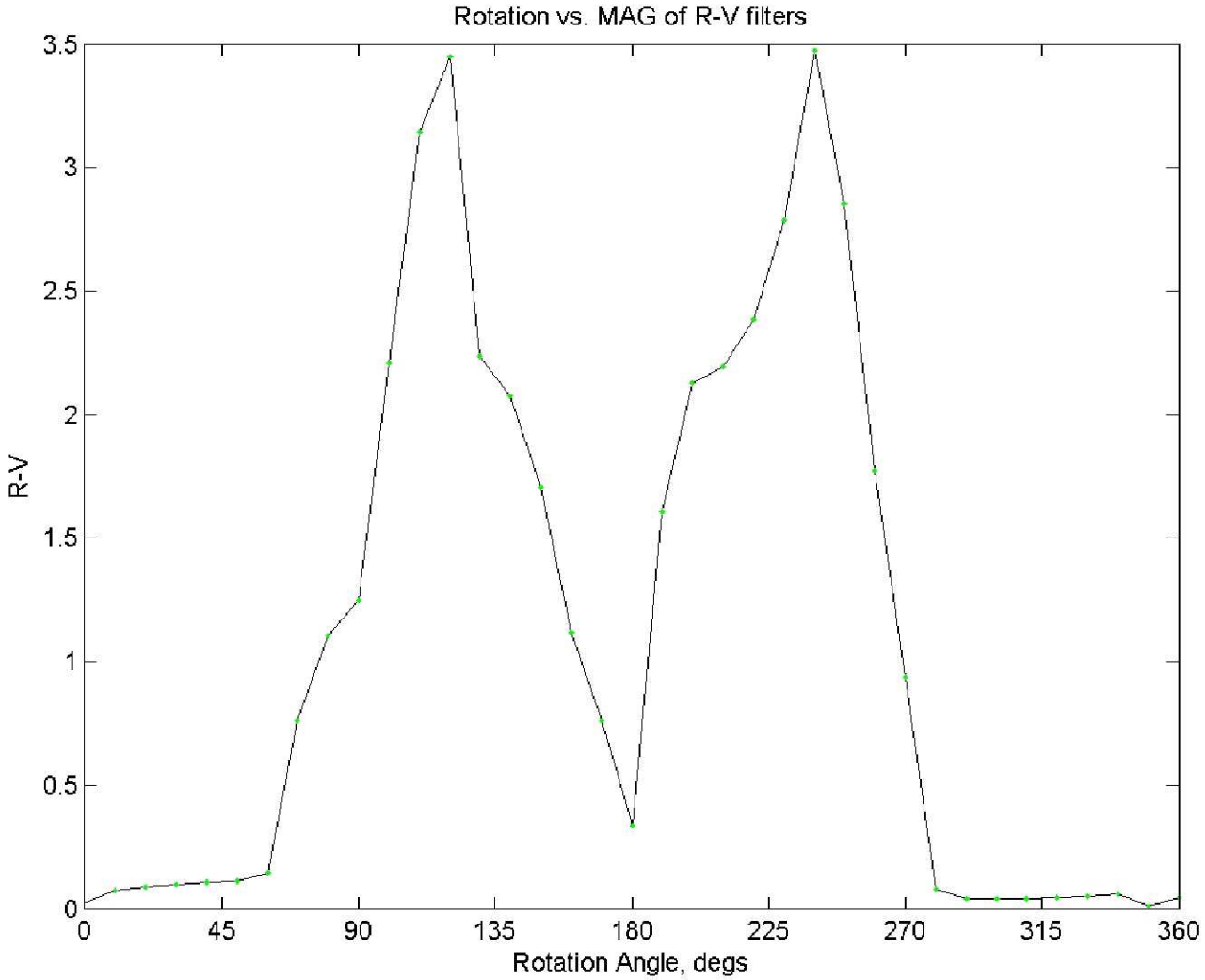

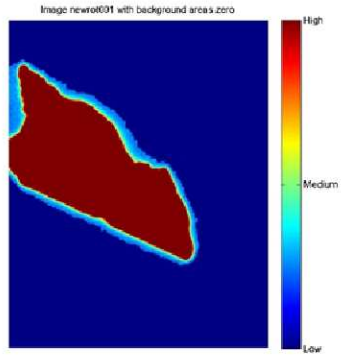

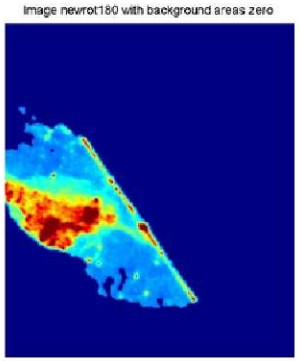

Solar Cell fragment

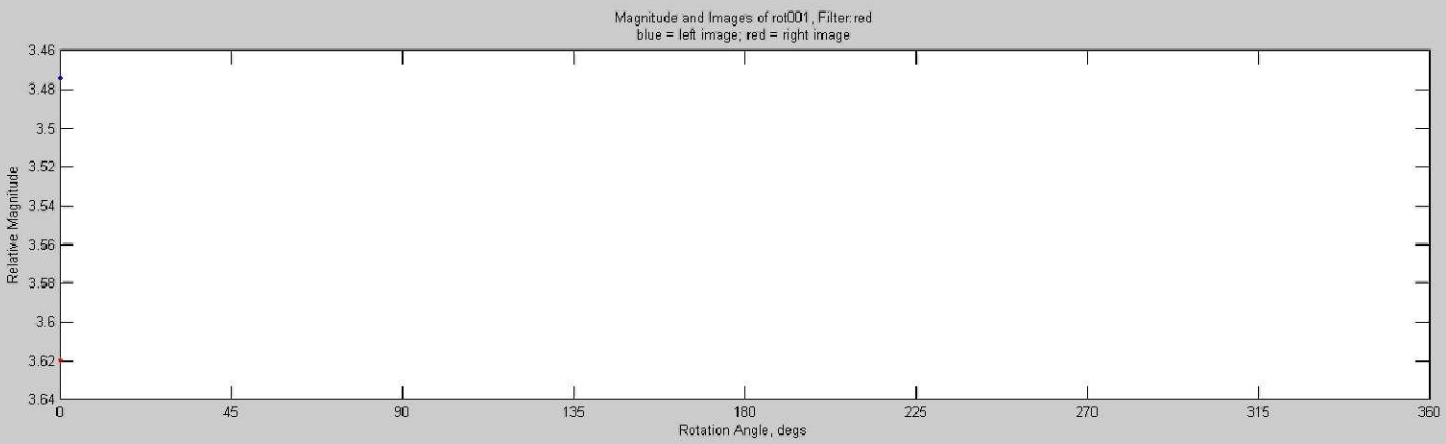

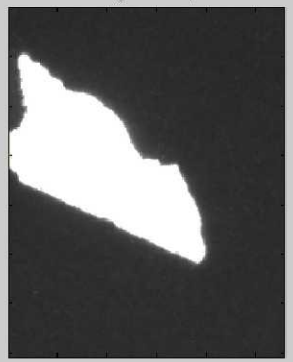

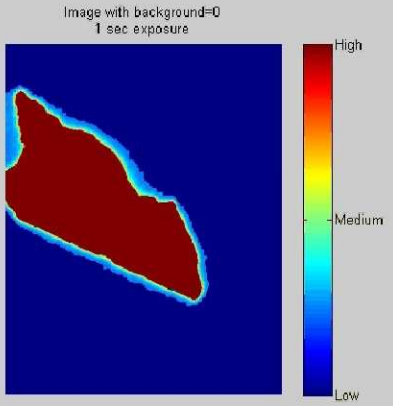

Intact solar panel

(solar cell top, aluminum honey comb sides, CFRP bottom)

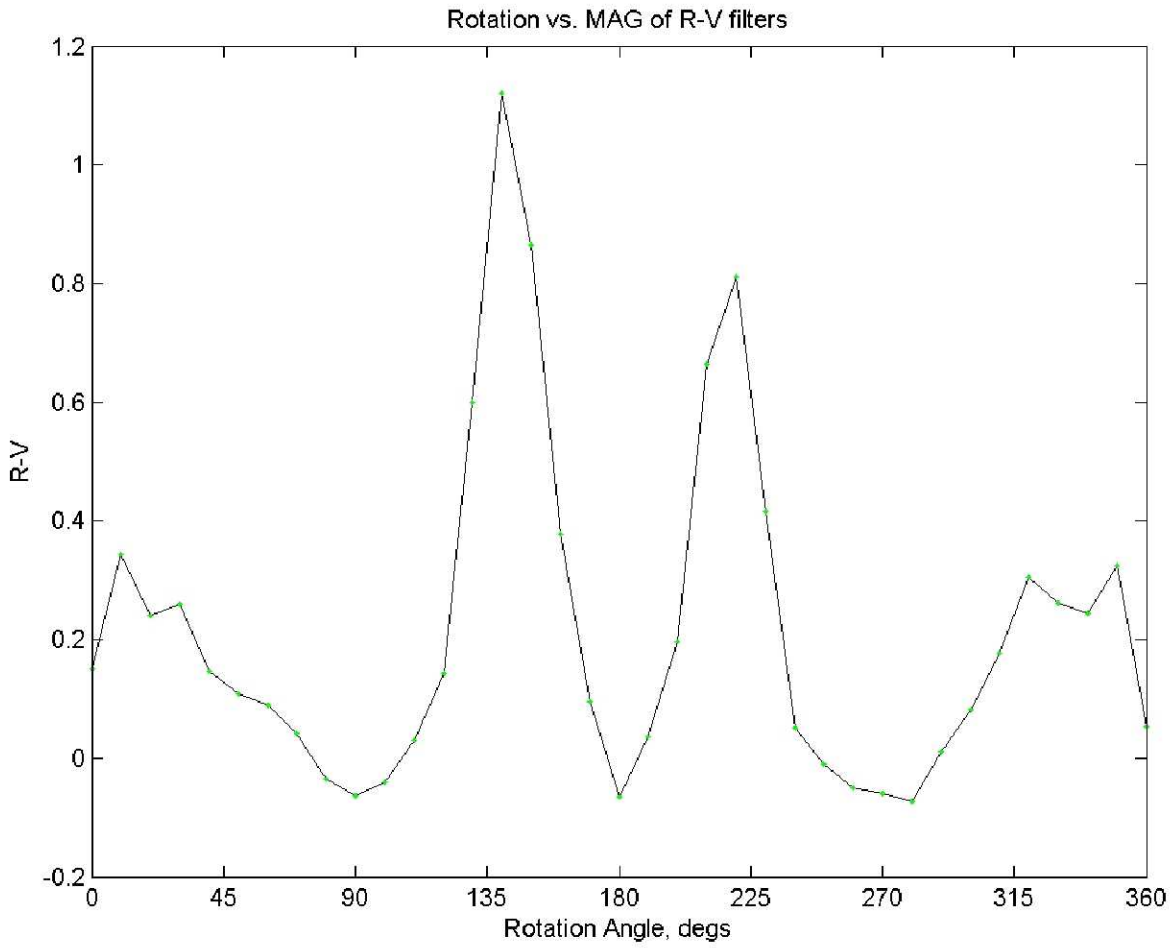

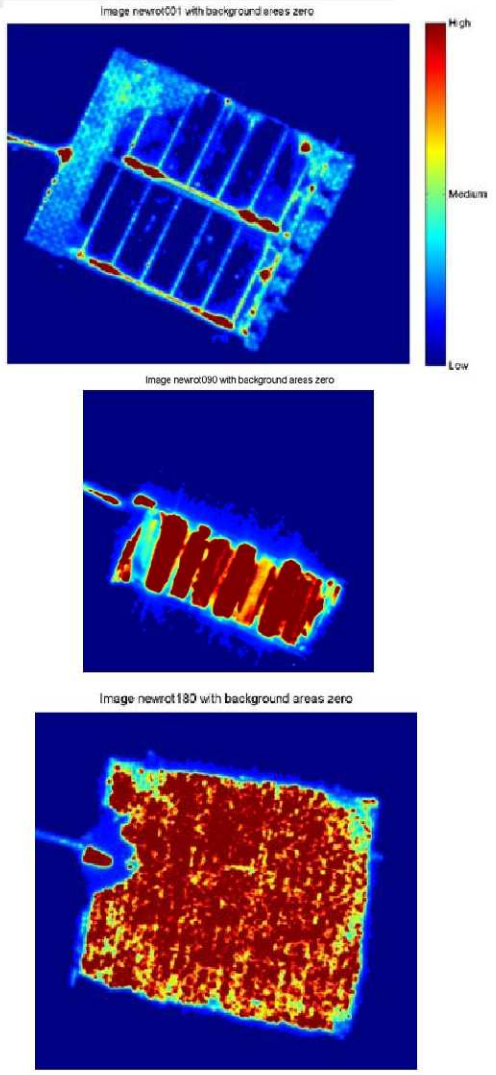

Intact Solar Panel

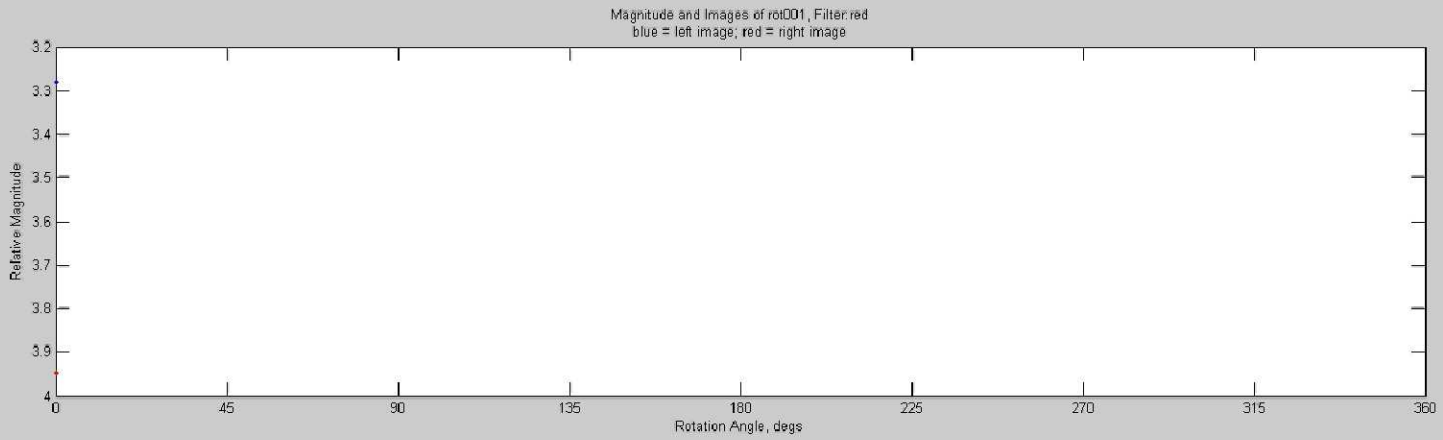

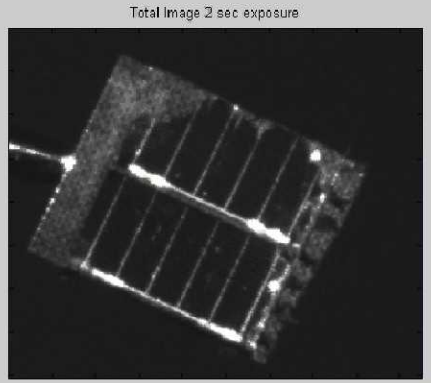

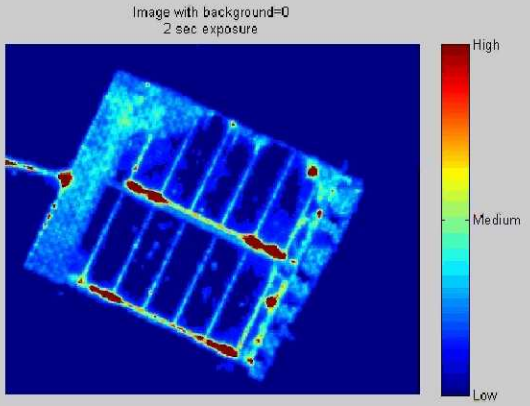


Telescope Measurements

AIUB telescope data of same target

A/m =

1.9 m2/kg

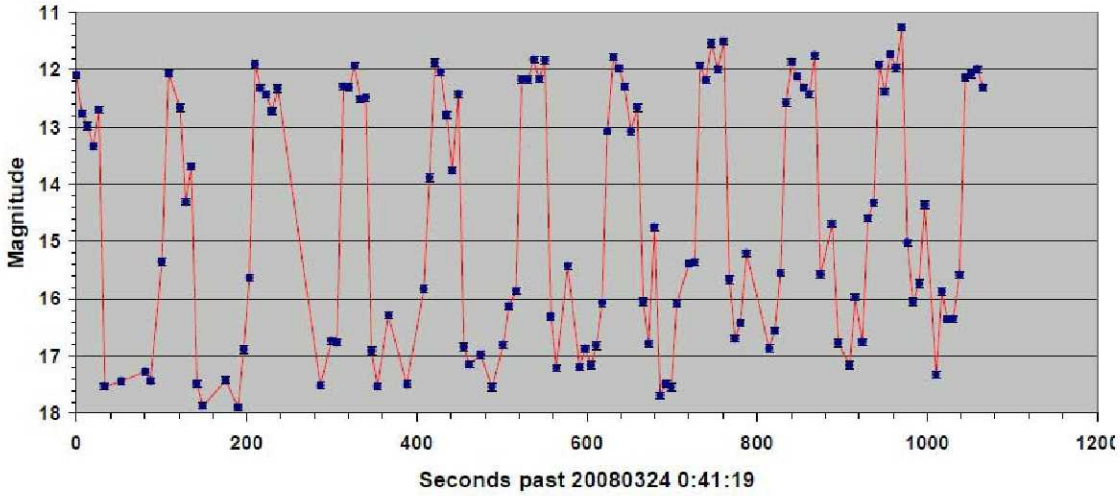

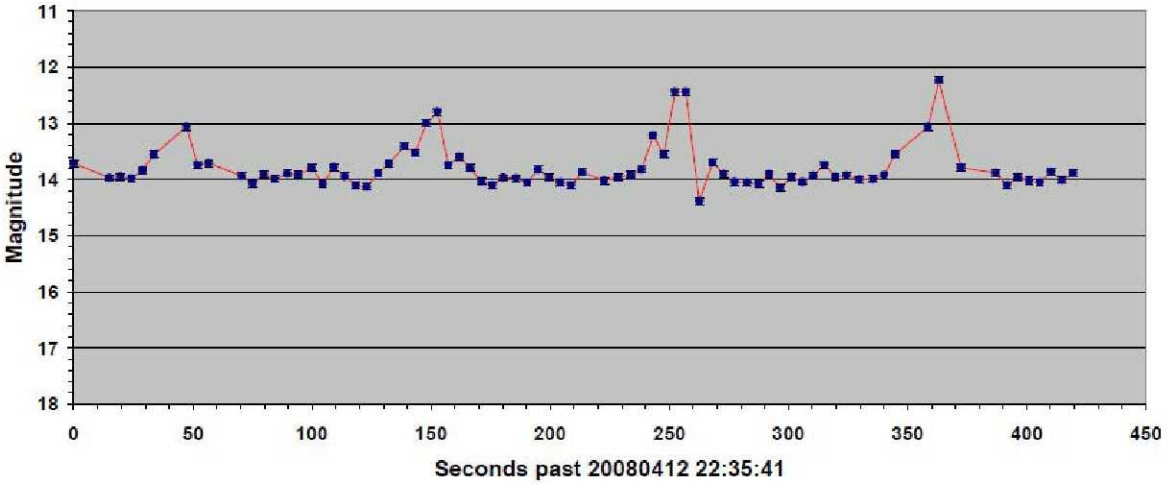

Possible correlation to: Intact MLI or Solar cell fragment

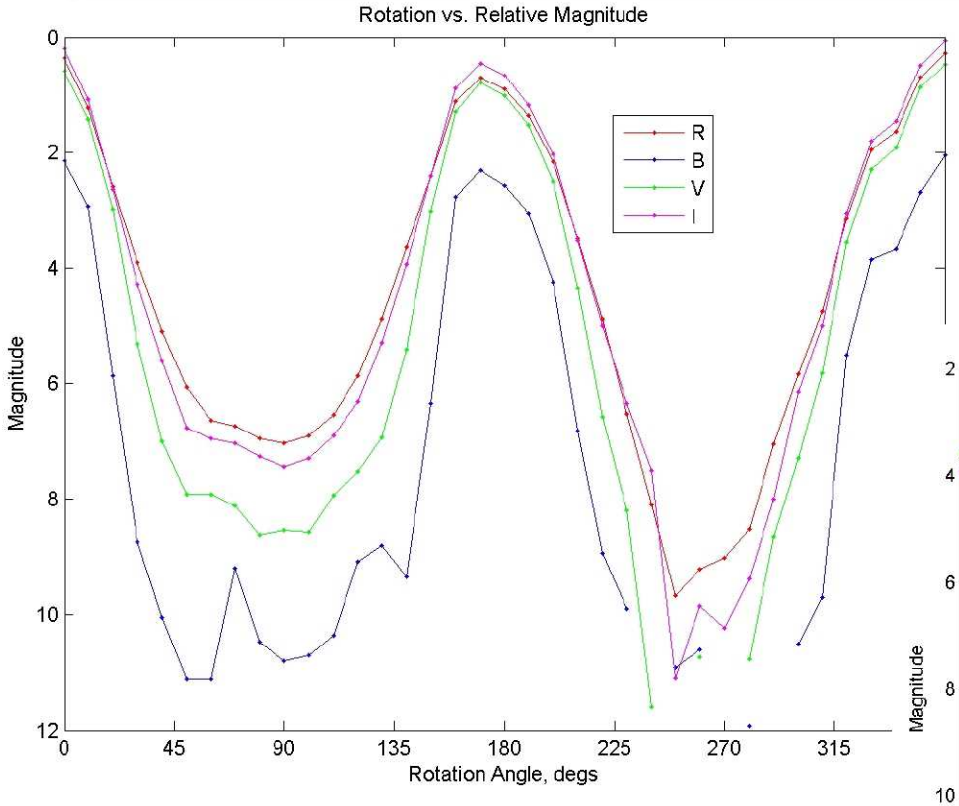

Intact MLI

A/m = 2.1 m^2/kg

Solar Cell

A/m = 1.0 m^2/kg

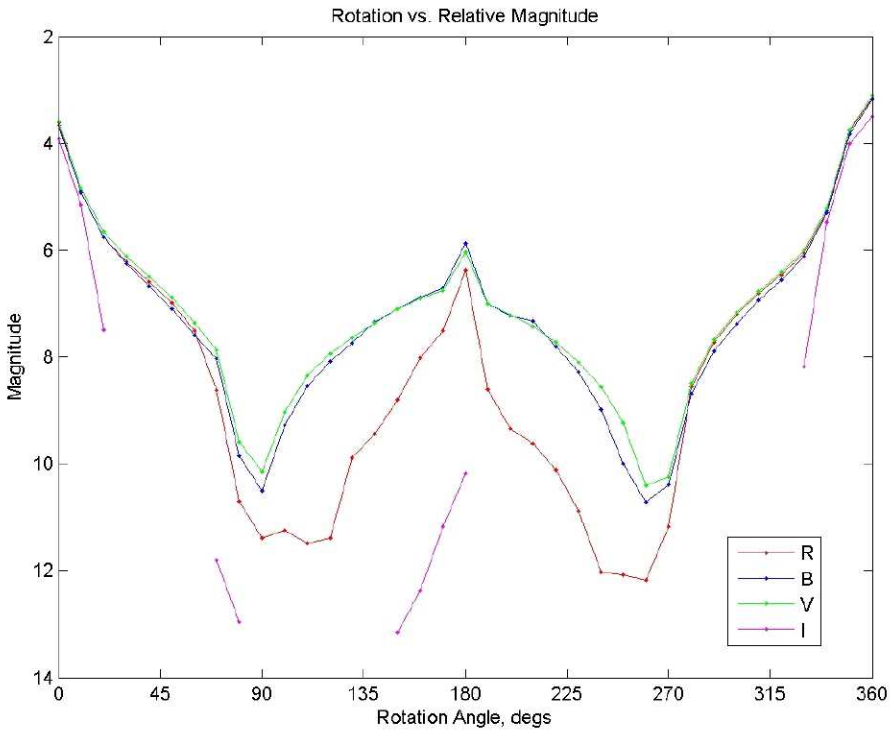

Photometry of stable UCT from CTIO 0.9 m

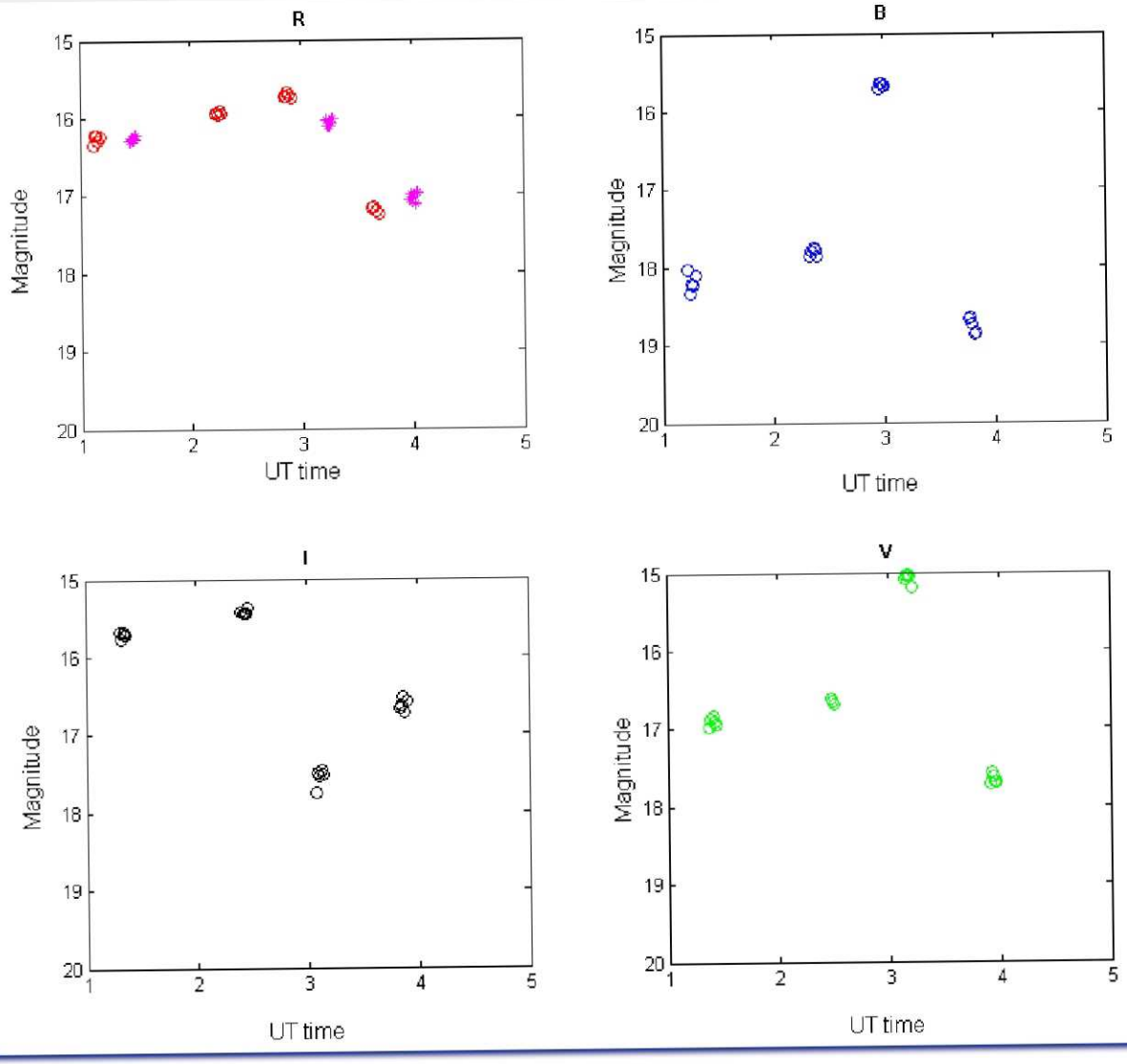

Similar behavior to MLI layers

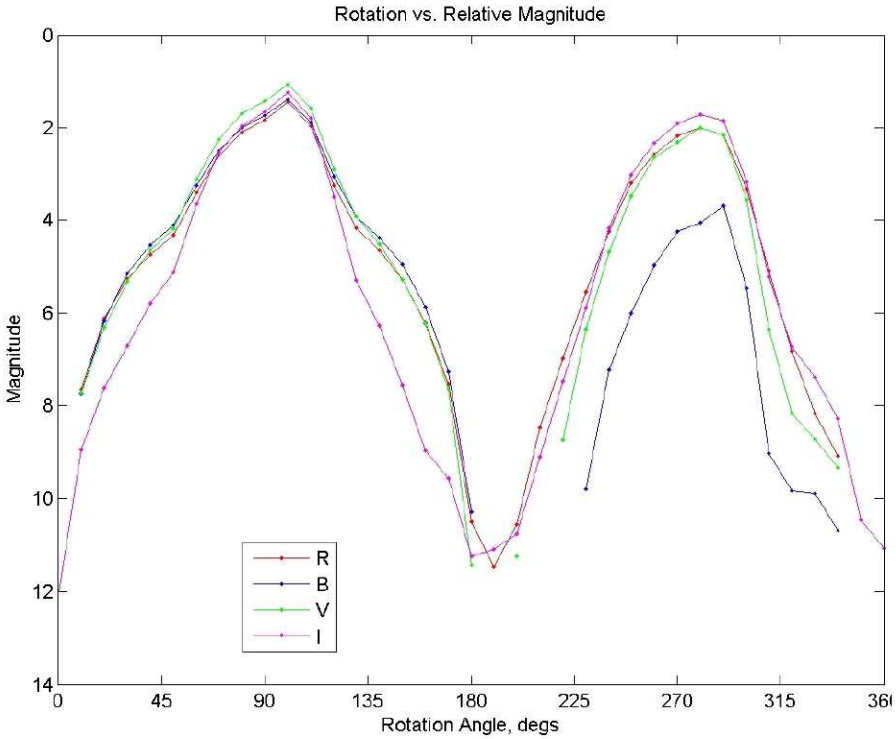

Space facing:

Copper colored Kapton illuminated first followed by aluminized Kapton

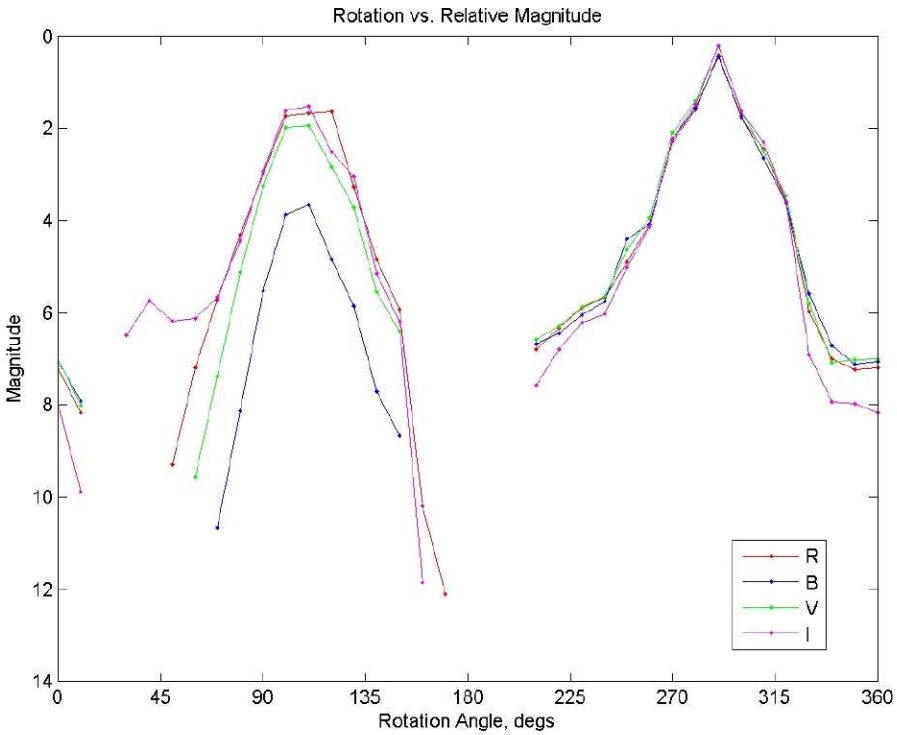

Spacecraft facing:

Aluminized Kapton illuminated first followed by copper-colored Kapton

Conclusions

- **In order to best compare laboratory and telescope data one must have two pieces of information: 1) the color lightcurve or color indices over time and 2) the A/m value.**
- **The suspected space fragment from the AUIB appeared to best match the MLI fragment, solely based upon the A/m value, but color information is needed to verify this preliminary assumption. If the object has a higher reflectance in the R than the B or V, then this object may in fact be MLI. Otherwise, the object could be a solar cell fragment if the reflection is higher in the B or V compared to the R filter.**
- **The UCT fragment observed on CTIO 0.9 m appeared stable between exposures but over the length of time appeared to change orientations leading to some insight on possible material identification. This behavior is also seen in the laboratory with the MLI layers as the aluminized Kapton becomes illuminated, the reflectance in the B and V filters increases significantly. Synchronous photometry of the same object in the R and B will aid in determining if the change was an artifact or a true change in the orientation of the object.**
- **The MLI fragment from the hypervelocity impact showed that the reflectance is reduced significantly due to the collision, leaving a thin film of suspected dark soot over the surface. This could imply that explosions in space that involve MLI may be undetectable at certain orientations.**
- **In an effort to best link laboratory data to telescope data, a wider sample of targets will be imported that include ground test fragments (CFRP,GFRP, plastics, wires, batteries, etc.).**
- **The phase angle was set as the initial basis and will soon be extended to 30° and 60° to best replicate the phase angles of other telescope observations.**
- **We will continue to look for correlations with telescopic observations with the intent of the assessing the material characteristics of the orbital debris population and the threat posed.**


Thank You

Back-Ups

- **CCD:**
  - 9 x 9 µ, transparent gate FI, single port, 15 e- read noise @ 400kHz
  - Fixed gain 2.3 e-/ADU, 16-bit A/D converter
  - TE (Peltier effect) cooled

- **Spectrometer**
  - Triplet multi-channel spectrometer covering Visible (300-750 nm), NIR (750 nm-1.4 µ), and SWIR (1.4-2.5 µ) wavelengths
  - Uses a holographic diffraction grating sampling the range from 300-2500nm with 717 channels at ~3 nm increments

Quick Review of MLI

- **Multi-layered insulation (MLI)**
- **Generally composed of**
  - Space-facing Kapton (copper is outwards facing and aluminized faces interior)
  - Layers of Mylar with NOMEX netting
  - Beta cloth
  - Spacecraft-facing Kapton (copper is outwards facing and aluminized faces interior)

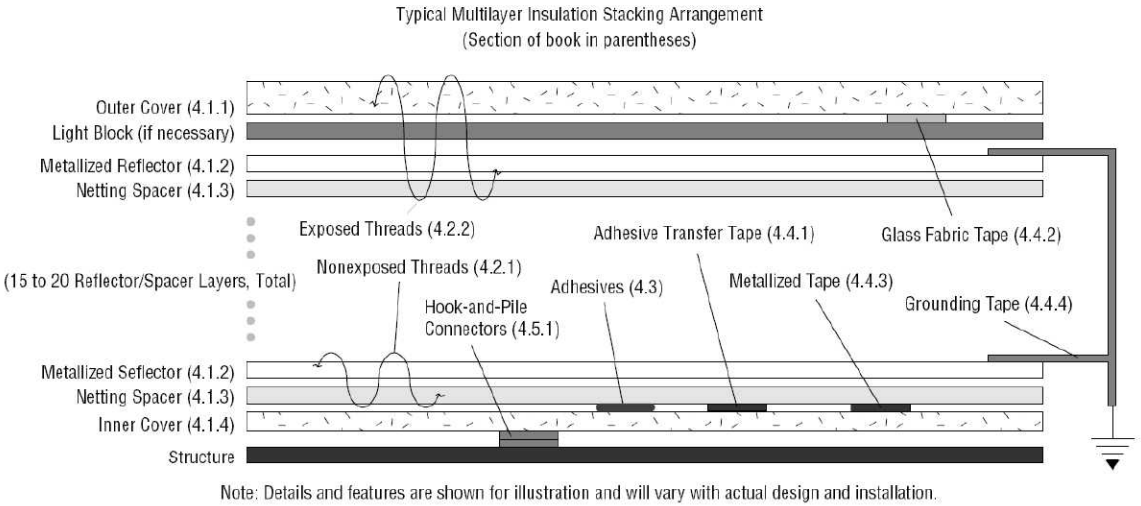

Figure 1. Schematic cross section depicts the key elements of an MLI blanket. Not all elements need be present in every design.